NASA CR 134896

EVALUATION OF MATERIALS AND DESIGN MODIFICATIONS FOR AIRCRAFT BRAKES

T.L. Ho, F.E. Kennedy, and M.B. Peterson

TRIBOLOGY LABORATORY
DEPARTMENT OF MECHANICAL ENGINEERING,
AERONAUTICAL ENGINEERING & MECHANICS
RENSSELAER POLYTECHNIC INSTITUTE
TROY, NEW YORK 12181

January 1975

Prepared for
AEROSPACE SAFETY RESEARCH AND DATA INSTITUTE
LEWIS RESEARCH CENTER
NATIONAL AERONAUTICS AND SPACE ADMINISTRATION
CLEVELAND, OHIO 44135

Under

NASA Grant NGR 33-018-152

H.W. Schmidt - Project Manager

R.C. Bill - Technical Adviser

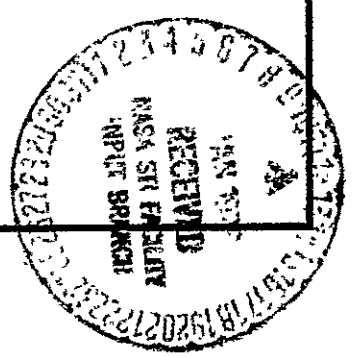

1. Report No.	2. Government Accession No.	3. Recipient's Catalog No.
CR 134896		N76-14464

4. Title and Subtitle	5. Report Date
Evaluation of Materials and Design Modifications for Aircraft Brakes	January 1975
	6. Performing Organization Code
7. Author(s)	8. Performing Organization Report No.
T.L. Ho, F.E. Kennedy and M.B. Peterson	
	10. Work Unit No.
9. Performing Organization Name and Address	
Rensselaer Polytechnic Institute Troy, New York 12181	11. Contract or Grant No. NGR 33-018-152
	13. Type of Report and Period Covered Contractor Report
12. Sponsoring Agency Name and Address	
National Aeronautics and Space Administration Washington, D.C. 20546	14. Sponsoring Agency Code

15 Supplementary Notes

Sponsored by Aerospace Safety Research and Data Institute, Lewis Research Center, Cleveland, Ohio 44135
H.W. Schmidt - Project Manager
R.C. Bill - Technical Adviser

16. Abstract

This report describes a test program which was carried out to evaluate several proposed design modifications and several new high-temperature friction materials for use in aircraft disk brakes. The evaluation program was carried out on a specially built test apparatus utilizing a disk brake and wheel half from a small jet aircraft. The apparatus enabled control of brake pressure, velocity and braking time. Tests were run under both constant and variable velocity conditions and covered a kinetic energy range similar to that encountered in aircraft brake service.

The results of the design evaluation program showed that some improvement in brake performance can be realized by making design changes in the components of the brake containing friction material. The improvement is not too significant, however.

The materials evaluation showed that two newly developed friction materials show potential for use in aircraft disk brakes. One of the materials is a nickel-based sintered composite, while the other is a molybdenum-based material. Both materials show much lower wear rates than conventional copper-based materials and are better able to withstand the high temperatures encountered during braking. Additional materials improvement is necessary, however, since both materials show a significant negative slope of the friction-velocity curve at low velocities.

17 Key Words (Suggested by Author(s))	18. Distribution Statement
Friction and Wear Brake Material Brake Design Brake Testing	Unclassified - unlimited

19. Security Classif. (of this report)	20. Security Classif. (of this page)
Unclassified	Unclassified

FOREWORD

This work was conducted as part of NASA Grant NGR 33-018-152 from the Office of University Affairs, Washington, D.C. 20546. Mr. Solomon Weiss of NASA's Aerospace Safety Research and Data Institute was the project monitor and Mr. R.L. Johnson, then Manager of NASA's Lubrication Research Branch, was the technical adviser at the time this report was prepared. Mr. H.W. Schmidt and Dr. R.C. Bill are the current project manager and technical adviser, respectively. Dr. F.F. Ling, Chairman of RPI's Department of Mechanical Engineering, Aeronautical Engineering & Mechanics, was the principal investigator.

Acknowledgement is made of the helpful suggestions made during the course of the investigation by Dr. Robert C. Bill of the U.S. Army Air Mobility R&D Laboratory at NASA-Lewis Research Center.

The authors also wish to acknowledge the generous donation of an aircraft brake by the Cessna Aircraft Company, the donation of metallurgical services by the Bendix Corporation, Friction Materials Division, and the donation of materials by Pure Carbon Company, Inc., the International Nickel Company, Inc., and DuPont Company.

The authors were assisted in the analysis of experimental data by Dr. V. Subbo Rao of R.P.I.

TABLE OF CONTENTS

SECTION 1

SUMMARY

This report describes a test program which was carried out to evaluate several proposed design modifications and several new high temperature friction materials for use in aircraft disk brakes. The evaluation program was carried out on a specially built test apparatus utilizing a disk brake and wheel half from a small jet aircraft. The apparatus enabled control of brake pressure, velocity, and braking time. Tests were run under both constant and variable velocity conditions and covered a kinetic energy range similar to that encountered in aircraft brake service.

The results of the design evaluation program showed that some improvement in brake performance can be realized by making design changes in the components of the brake containing friction material.

The materials evaluation showed that two newly developed friction materials show potential for use in aircraft disk brakes. One of the materials is a nickel-based sintered composite, while the other is a molybdenum-based material. Both materials show much lower wear rates than conventional copper-based materials and are better able to withstand the high temperatures encountered during braking. Additional materials improvement is necessary, however, since both materials show a significant negative slope of the friction-velocity curve at low velocities.

SECTION 2

INTRODUCTION

The disk brakes used on jet aircraft are called upon to transform large amounts of kinetic energy to thermal energy in a very short time. The performance of these high energy brakes is important for a variety of reasons - economy, passenger comfort, and, most important, safety. In order to improve brake performance, research has been carried out in recent years in a number of laboratories (Refs.1-7). Most of this research, however, has been of a proprietary nature, with little dissemination of the research results to the technical community.

For the past few years a research program has been in progress at Rensselaer Polytechnic Institute, sponsored by a grant from NASA's Aerospace Safety Research and Data Institute, for the purpose of investigating aircraft disk brakes, especially from the point of view of safety. Initial phases of the research program included an experimental study of the friction and wear behavior of typical brake friction materials (Ref.1) and an analytical investigation of the thermomechanical behavior of the brake components (Ref.2). An experimental investigation of the temperatures, friction, wear, and contact conditions in typical disk brake friction pads was also performed (Ref.3).

The results of the initial, more fundamental studies were then applied to the development of brake modifications that could improve the performance of aircraft disk brakes. New high-temperature friction materials have been developed which seem to perform better under high energy sliding conditions than do the more commonly used materials (Ref.4). Changes in friction pad designs have also been proposed which could enable better braking performance to be achieved with existing friction materials (Ref.3).

The proposed materials and design modifications performed well in idealized laboratory tests in which small specimens were tested under constant velocity sliding conditions. It was felt that a combination of the new friction materials and the improved designs could result in safer, longer lasting, more reliable disk brakes for aircraft. In order to test this concept, it was necessary to incorporate each proposed modification into an actual disk brake and evaluate it

under conditions similar to those encountered in service. This report presents the results of that evaluation program.

The test program was composed of two phases: a comparative evaluation of design modifications proposed earlier (Ref.3), and a comparative evaluation of new high temperature friction materials developed either in earlier phases of this project (Ref.4) or in a separate materials development project at NASA-Lewis Research Center (Ref.5). Each material or design modification was tested separately under a variety of controlled, simulated service conditions, with measurements being made of friction wear, sliding surface temperature, and surface conditions. The test results were compared with results of similar tests on a standard brake configuration employing conventional copper-base friction material.

The program of tests was carried out on a specially built test apparatus which enabled control of brake pressure, velocity and braking time. Tests were run under both constant and variable velocity conditions and covered a kinetic energy range similar to that encountered in service.

SECTION 3

TEST FACILITY

A test facility was constructed especially for use in this investigation in an annex to the Tribology Laboratory at Rensselaer Polytechnic Institute. The equipment in this laboratory, shown in Figure 1, was purchased and assembled especially for use in the evaluation of brake systems. In contrast to the very large and expensive test dynamometers used in most brake and wheel testing, this test facility is relatively simple and inexpensive, but is capable of giving a great deal of information from brake tests under a wide variety of test conditions.

Rotational power is provided to the brake by a 75-KW AC electric motor coupled to a 175-KW water-cooled eddy current coupling. These units, with their electrical controls, provide a source of constant torque at controlled speeds ranging from zero to 1750 rpm.

A complete brake from a small jet aircraft, with a wheel half, was donated by an aircraft manufacturer for use in the brake studies. A modified version of the brake was used in the investigation, having one rotating disk instead of the normal two. [The design of the brake's stationary and rotating disks varied between tests as part of the design evaluation phase of the study. These designs will be discussed in later sections of this report. A sectional view of a typical brake system is shown in Figure 2.]

The stationary brake components were attached to a stationary steel shaft, carefully aligned with the rotating components. A regulated oil-lubricated compressed air supply was used to actuate the brake. The pneumatic circuit was activated by a solenoid valve, with the duration of the brake application being controlled by a timer switch.

The brake test rig was equipped with a number of instruments for monitoring test information. The monitoring equipment included the following:

1. A semiconductor pressure transducer for monitoring air pressure in the brake hydraulic system.
2. A strain gage torquemeter, consisting of four strain gages mounted parallel to the principal axes on the stationary shaft, for monitoring frictional torque.

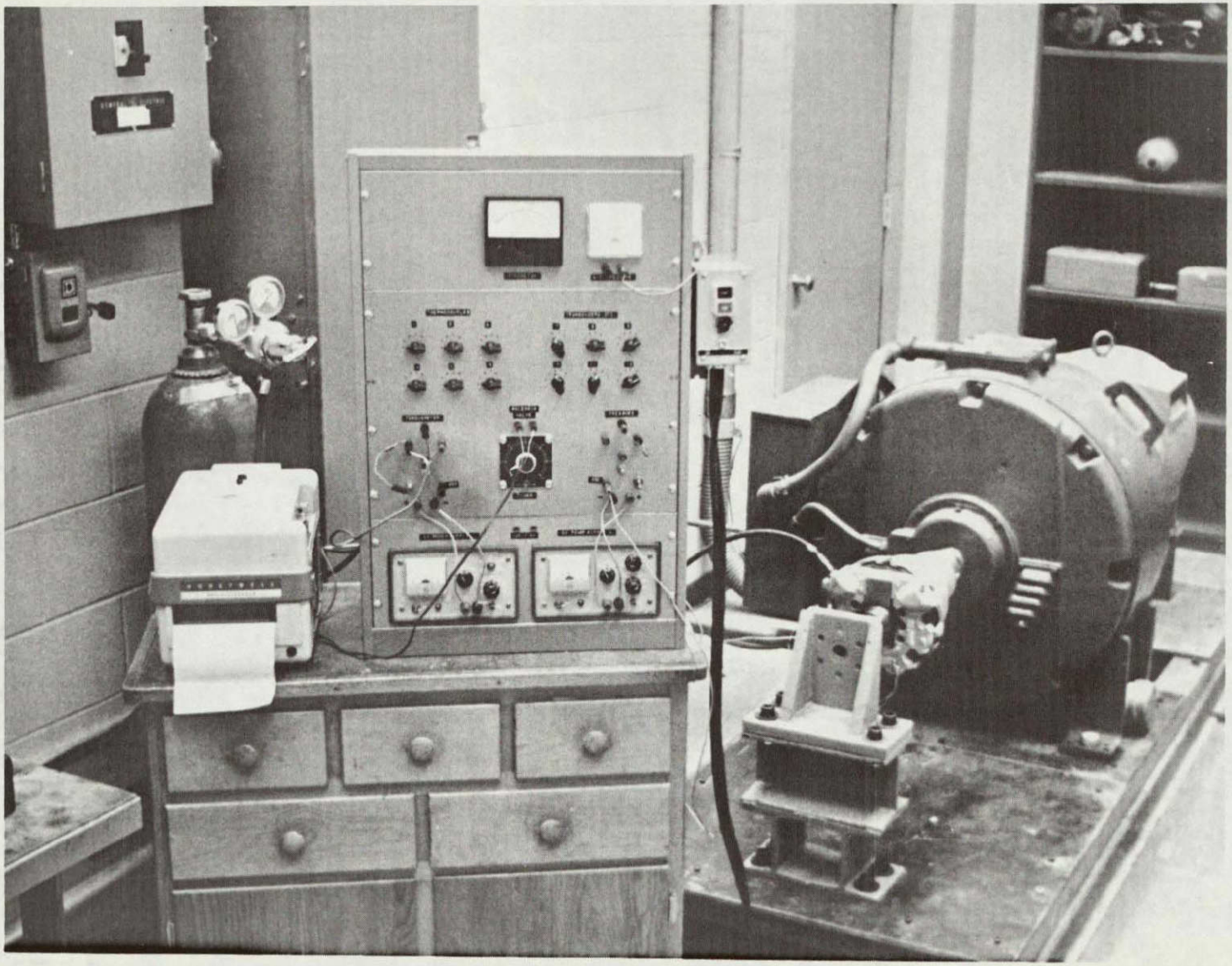

Figure 1 Photograph of Test Apparatus for Brake Evaluation (Protective Shield Removed)

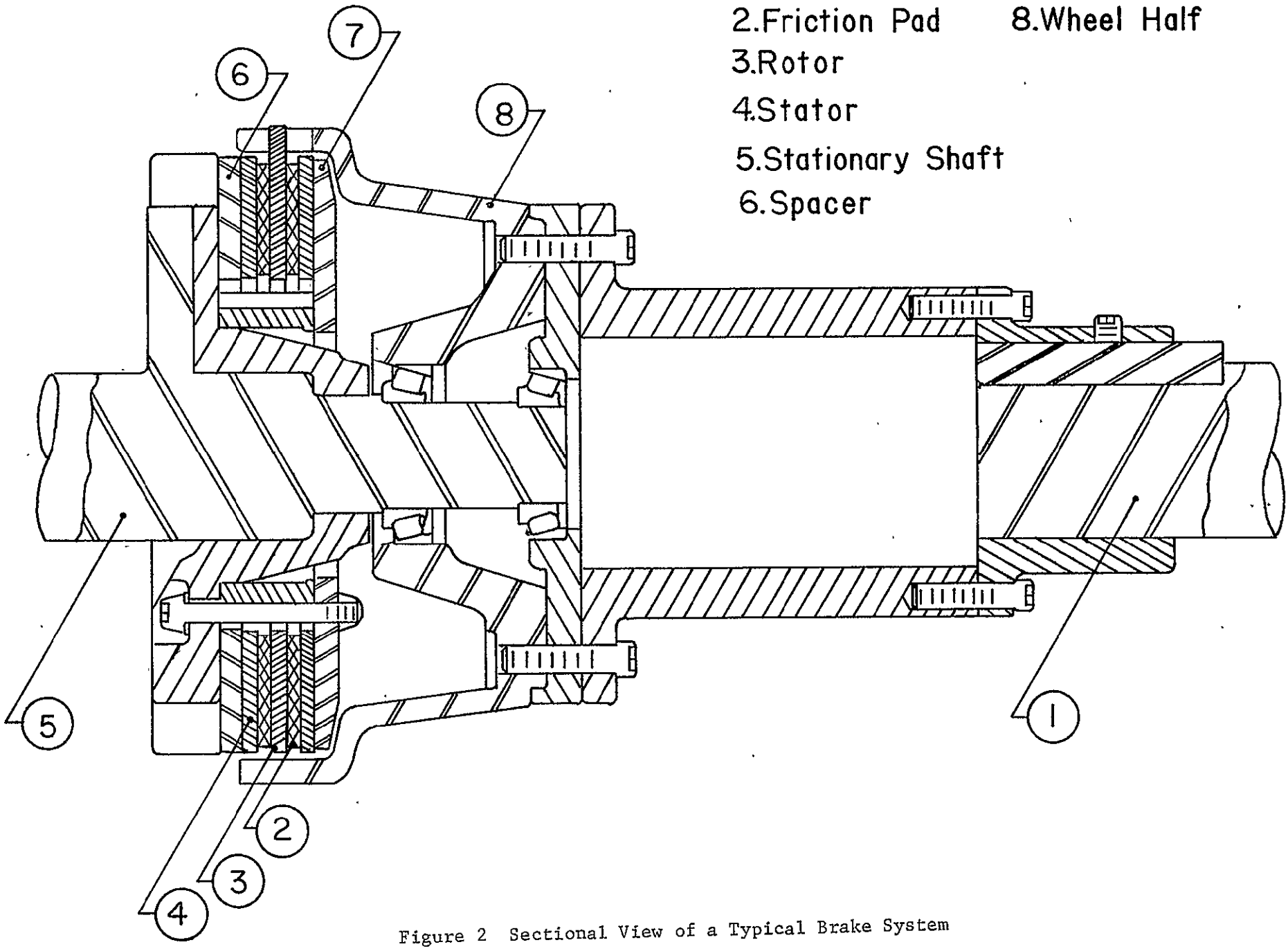

Figure 2 Sectional View of a Typical Brake System

3. A tachometer for monitoring rotational velocity of the brake rotor.
4. A timer for regulating the length of the brake application.
5. Chromel-alumel thermocouples, located in the brake's stationary components, for measuring near-surface brake temperatures. Up to eight thermocouples were inserted through the rear of the stator components to within .25 mm to 1.59 mm of the friction surface at various locations inside the brake, enabling determination of transient radial and circumferential temperature distribution close to the sliding interface.

All electrical signals from the monitoring devices were continuously recorded on a 12-channel oscillograph, with some panel meters also being used for monitoring output signals. All devices were carefully calibrated before the test program and the calibrations were checked occasionally during the investigation.

A schematic diagram showing the test equipment is included as Figure 3.

1 – WHEEL HALF

2 – DISC BRAKE

3 – PRESSURE TRANSDUCER

4 – STRAIN GAGE TORQUEMETER

5 – THERMOCOUPLES

6 – TACHOMETER

7 – SOLENOID VALVE

8 – REGULATED COMPRESSED AIR SUPPLY

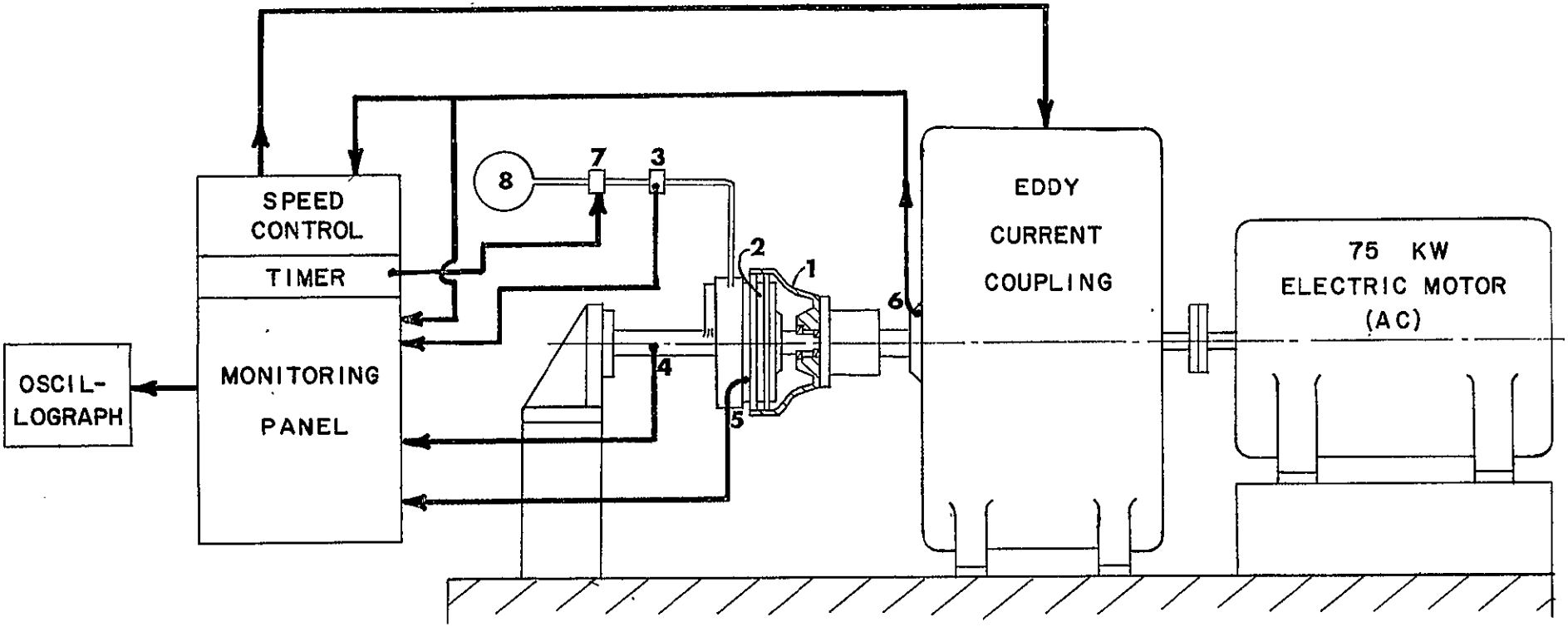

Figure 3 Schematic Diagram of Test Equipment

SECTION 4

EXPERIMENTAL PROCEDURE

There is no well-defined procedure for use in the evaluation of brake systems. The desirable characteristics of high energy disk brakes include the ability to dissipate a large amount of kinetic energy with minimum wear, good frictional behavior, and relatively low brake temperatures. Any proper brake evaluation should include a determination of these brake characteristics over a wide range of conditions similar to those encountered in service.

For the purpose of this investigation, a comparative type of evaluation was chosen. Eight different single rotor - two stator brakes were tested, with each being tested under similar test conditions. Two of the brake systems were standard configurations similar to those used in modern jet aircraft. The results of the tests on these brakes served as a basis for the comparative evaluation of the remaining seven brakes. Each of the other brakes contained a modification, either in friction material or in design, from the standard configurations. Relevant information about the eight brakes evaluated is given in Table 1. Brakes A and E in the table are standard disk brake configurations. The brake design and materials will be discussed in more detail in later sections of this report.

The testing program for each of the eight brake systems consisted of six test series, with five test runs in each series. The test conditions were kept the same for all test runs in each series, but varied considerably between series in an attempt to cover the wide range of braking conditions encountered in normal service. The various conditions under which each brake was tested will be discussed in detail in later sections of the report.

The program of tests on each brake began with new friction material on the brake's friction surfaces and with either new or newly ground and cleaned steel mating surfaces. The same components were then used for all six series of tests on the brake. The friction material components were weighed carefully before the first tests to provide a basis for wear rate determination. During a test series the brake remained untouched, before being disassembled after completion of the series for weighing of friction components and examination of sliding surfaces. Except for removal of loose wear debris, no cleaning of either rotor or stator was done during testing of a brake.

TABLE 1

PRINCIPAL CHARACTERISTICS OF BRAKES BEING EVALUATED

Brake Designation	Friction Material	Location of Friction Material	Geometry of Friction Material
A	Cu-base	Rotor	Annulus
B	Cu-base	Rotor	Annulus with slots
C	Ni-base	Stator	Buttons
D	Mo-base	Stator	Buttons
E	Cu-base	Stator	Circular pads
F	Ni-base	Stator	Circular pads
G	Mo-base	Stator	Circular pads
H	Carbon	Stator	Circular pads

The other sliding material for all cases was a high temperature alloy of steel (1722 AS).

Before each test run the air pressure regulator, interval timer, and speed controller were set at their approximate initial values. Velocity changes during the variable velocity test runs were accomplished by manual adjustment of the speed controller in order to obtain constant deceleration rates.

Oscillograph traces were recorded continuously during each test run for the output signals from tachometer, torquemeter, pressure transducer, and all thermocouples.

At the conclusion of each test run the motor and eddy current coupling unit were shut off and the brake components were allowed to cool to room temperature (approximately 22°C) before the next run. A fan was used to direct air at the brake between some of the test runs in order to reduce the length of time required to bring the brake components to ambient temperature. No cooling measures were employed during the braking tests.

SECTION 5

DESIGN EVALUATION

5.1 Design Configurations and Test Conditions

Four different brake configurations were examined in the design evaluation phase of this project. A brief description of each follows.

Annular Brake. This brake is a conventional brake configuration used in the disk brakes of a number of small jet aircraft. The friction material is in the shape of an annulus and is bonded to both sides of a steel rotor disk, as shown in Figure 4. The friction material used in this brake was a commercial, sintered, copper-based brake material. Both brake stators consisted of twelve trapezoidal pads rigidly fastened to an annular disk, as shown in Figure 5. The pads were made of a high temperature alloy of steel (1722 AS) and the disks were made of a high strength steel alloy. The sliding surfaces of the pads were ground finished. One of the stator disks served as the brake's back plate and the other served as the pressure plate. A spacer was located between the pressure plate and the hydraulic pistons. The spacer was necessary since the brake had been modified from a two rotor to a single rotor brake for the purpose of this test program. Seven thermocouples were installed in the brake's stators, with four in the back plate and three in the pressure plate. The locations of the thermocouples are shown in Figure 5. Each of the thermocouples was mounted in a small hole drilled in the rear (non-contacting) face of the stator disk to within .25 - 1.0 mm of the contacting surface of the stator. Porcelain cement with high thermal shock resistance was used to hold the thermocouples in place during the tests.

This brake configuration was used only for brake A (see Table 1).

Slotted Annular Brake. This brake was nearly the same as the annular brake described above. The only exception was the presence of slots cut through the friction material on both sides of the rotor. Twenty-one equally spaced slots, each 6.4 mm wide were milled on each face of the rotor, as shown by the dotted lines in Figure 4. The purpose of the slots was to test the conclusion of an earlier study (Ref.3), which indicated that a radial slot cut into the sliding surface of a brake pad resulted in decreased surface temperatures and wear rate during braking. It

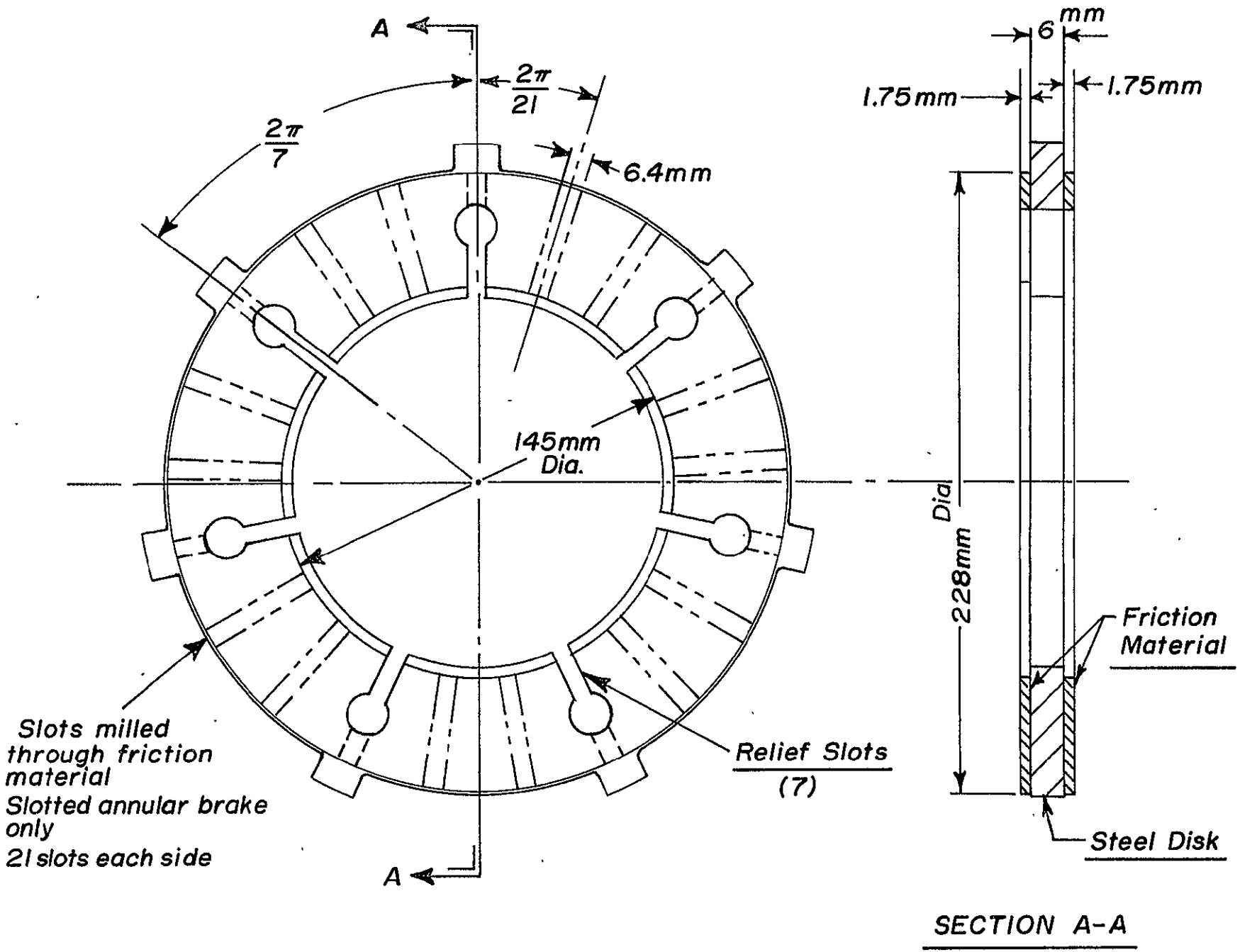

Figure 4 Rotor Disk Used in Annular and Slotted Annular Brakes

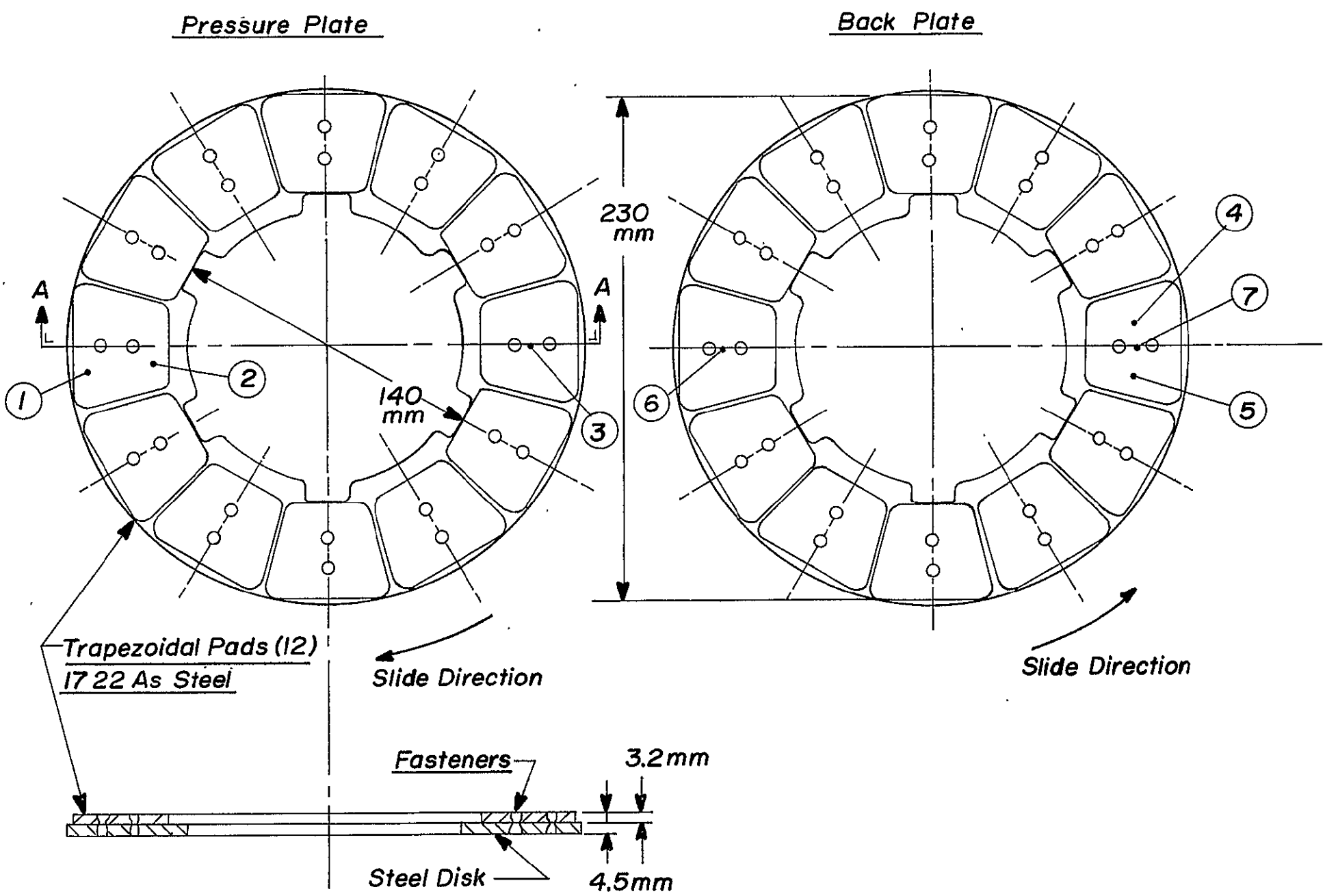

Figure 5 Stator Disks for Annular and Slotted Annular Brakes, Showing Locations of Thermocouples

was felt that such a slot enabled removal of abrasive wear particles from the sliding surface and improved the ability of the friction material to adjust to nonuniform thermal deformation of the friction surface.

The stators of this brake had the same configuration as for the annular brake discussed above, and the thermocouple positions remained the same.

This slotted annulus configuration was employed only in brake B (Table 1).

Button Brake. The third brake configuration investigated consisted of a distribution of small (19 mm diameter) buttons of friction material on the stator disks, as shown in Figure 6. The buttons were individually press-formed and, after sintering, were shrink-fit into holes in two annular stator disks. Each of the two aluminum stators held thirty-two buttons of friction material. The button design was proposed earlier (Ref.4) after an experimental study (Ref.3) had shown that contact occurs only at isolated locations on a brake's friction surface, resulting in nonuniform thermal deformation and concentrated wear. It was felt that the button design could allow more uniform contact conditions, lower brake temperatures, and, hopefully, lower wear.

Thermocouples were positioned inside buttons at several locations on each stator. Holes were drilled at the center of rear (noncontacting) face of the buttons to within 1.59 mm of the friction surface and the thermocouples were mounted in the holes using porcelain cement. Seven thermocouples were utilized, with the thermocouple locations shown in Figure 6.

The rotor for the button brake was machined from 1722 AS steel and is shown in Figure 7. The sliding surfaces were ground finished and the disk was heat treated to a hardness of Rc 44 - Rc 50. This heat treatment was used on Brakes A and B also.

Two different versions of the button brake were tested. Brake C used buttons composed of a nickel-based friction material, while Brake D utilized molybdenum-based friction material buttons. Both friction materials were developed in earlier phases of this project (Ref.4) and will be discussed in more detail in Section 6 of this report.

Pad Brake. The final brake configuration studied was one employing pads of friction material on the brake stators. This is another standard commercial

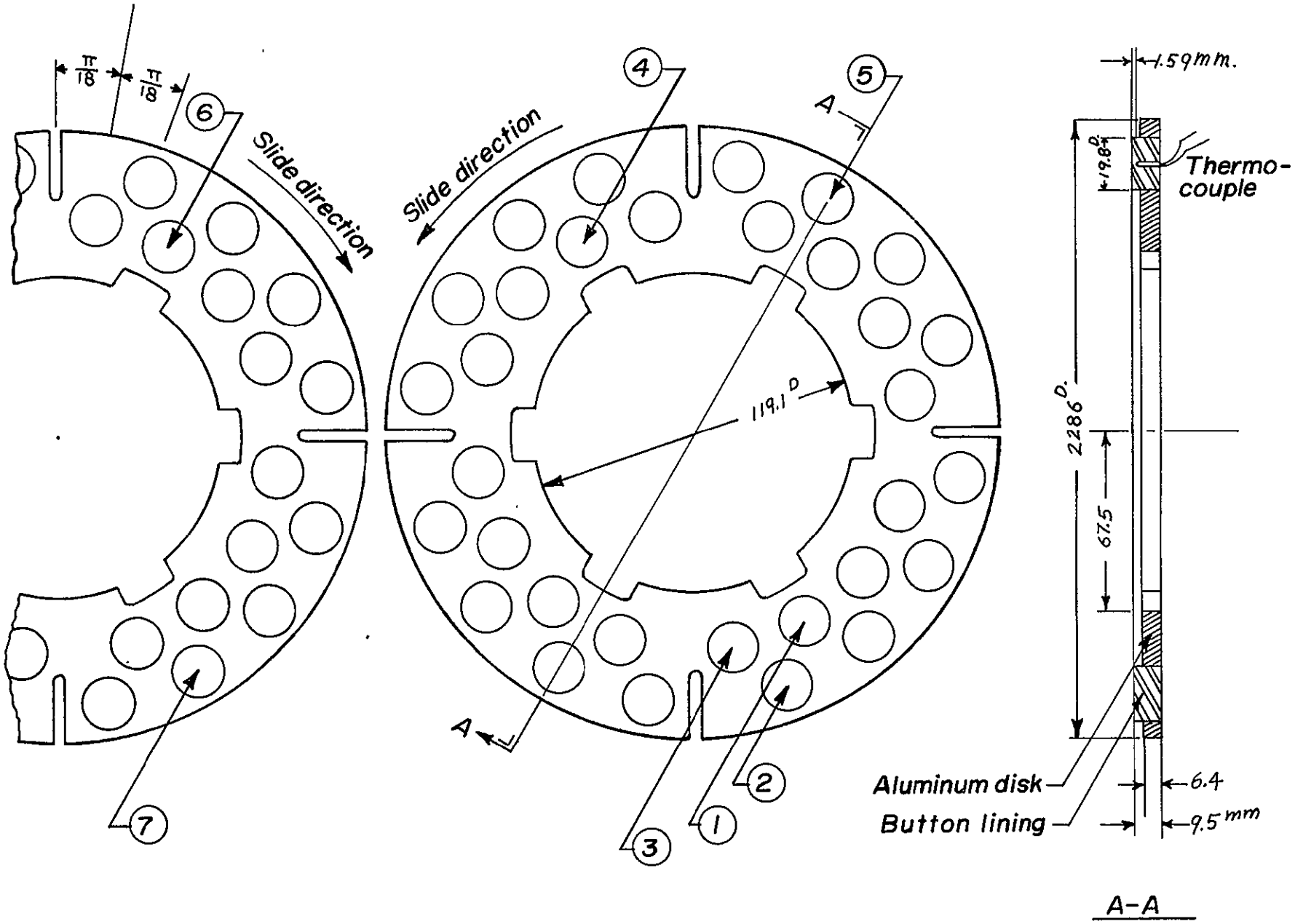

Figure 6 Location of Thermocouples in Button Brake Stators

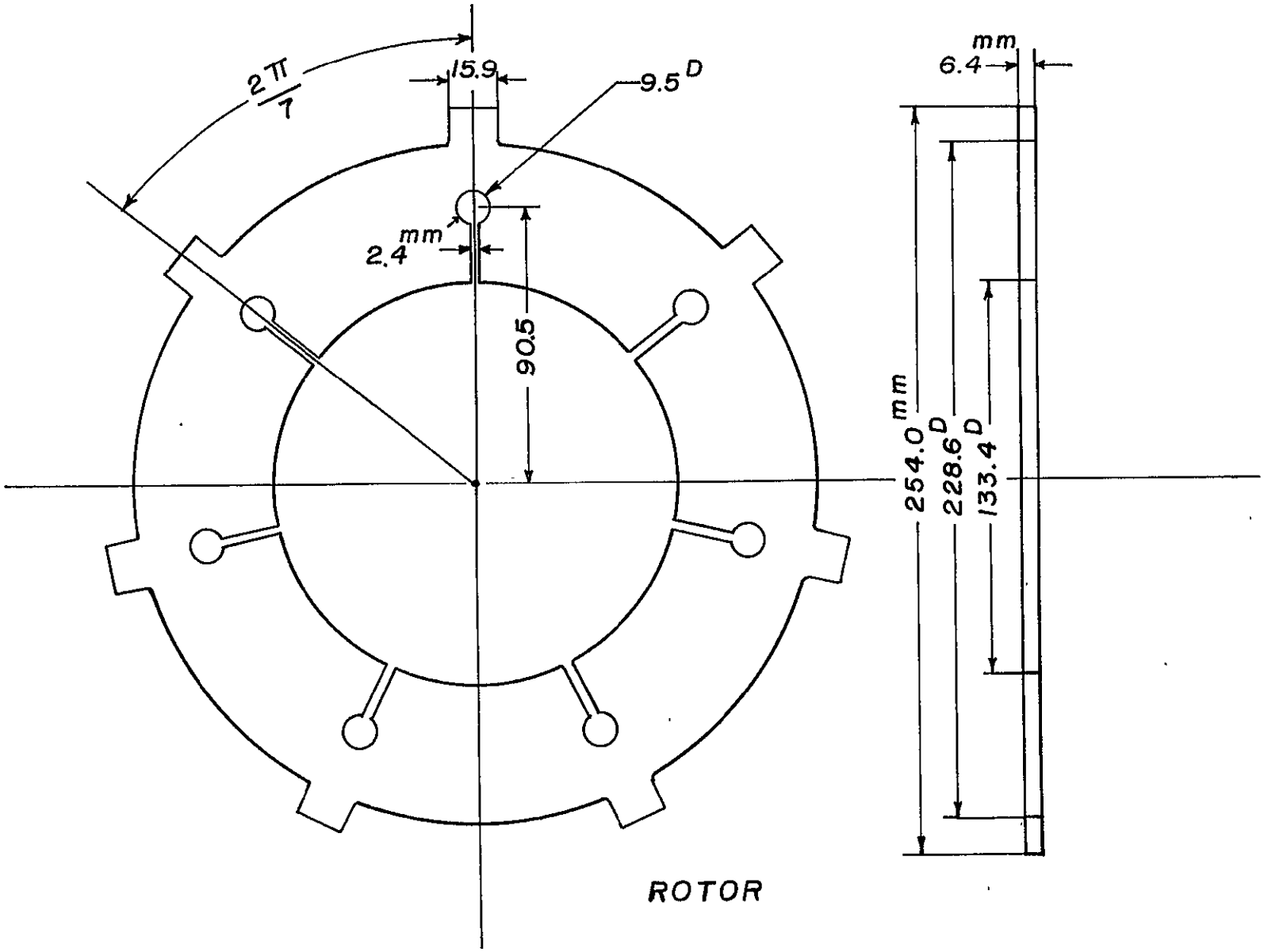

Figure 7 Diagram of Rotor Disk for Button and Pad Brakes

configuration used on many jet aircraft. The rotor for this brake was the same design and material as that described above for the button brake and shown in Figure 7. A new rotor was used for each brake tested.

The friction pads for this brake were mounted rigidly to one side of each of the two brake stator disks, with twelve pads on each stator, as shown in Figure 8. The stator disk was made of carbon steel and had interior splines for anchoring to the torque tube. The friction pads were circular in shape and consisted of friction material contained in a steel cup. A sketch of a typical friction pad is shown in Figure 9. The pads were rigidly attached to the stator disk by a rivet fastener at the center of the pad.

The pad brake configuration was used for four of the brakes tested, labeled E through H in Table 1. Each of these four brakes had the same dimensions, but used a different friction material in the friction pads. With some of the materials a thin steel mesh was used between the sintered material and the steel cup to aid in bonding the material to the cup. The different friction materials will be discussed in more detail in Section 6 of this report.

Seven thermocouples were used in monitoring the near-surface temperatures in the pad brake. The thermocouple locations are shown in Figure 10. Holes for the thermocouples were drilled through the rear face of the stator disk and into the friction pads, stopping within 0.5 - 1.59 mm of the sliding surface. The thermocouples were mounted in the holes using porcelain cement.

It should be noted that each of the above rotor-stator configurations was designed to be used with the same aircraft brake and inside the same wheel half. Thus, the major dimensions of each of the designs are similar. The major difference is in the shape and size of the nominal sliding surface of the friction material. The annular brake had 216.3 cm^2 of nominal rubbing area of friction material, the slotted annular brake had 174.0 cm^2, the button brake pad had 91.2 cm^2 and the pad brake had 160.6 cm^2.

Test Conditions. The test conditions used in the testing of each brake configuration are given in Table 2. A number of different conditions were employed in order to cover the wide range of conditions encountered in brake service. Some of the tests, such as series 4, 8, and 9, were meant to simulate actual

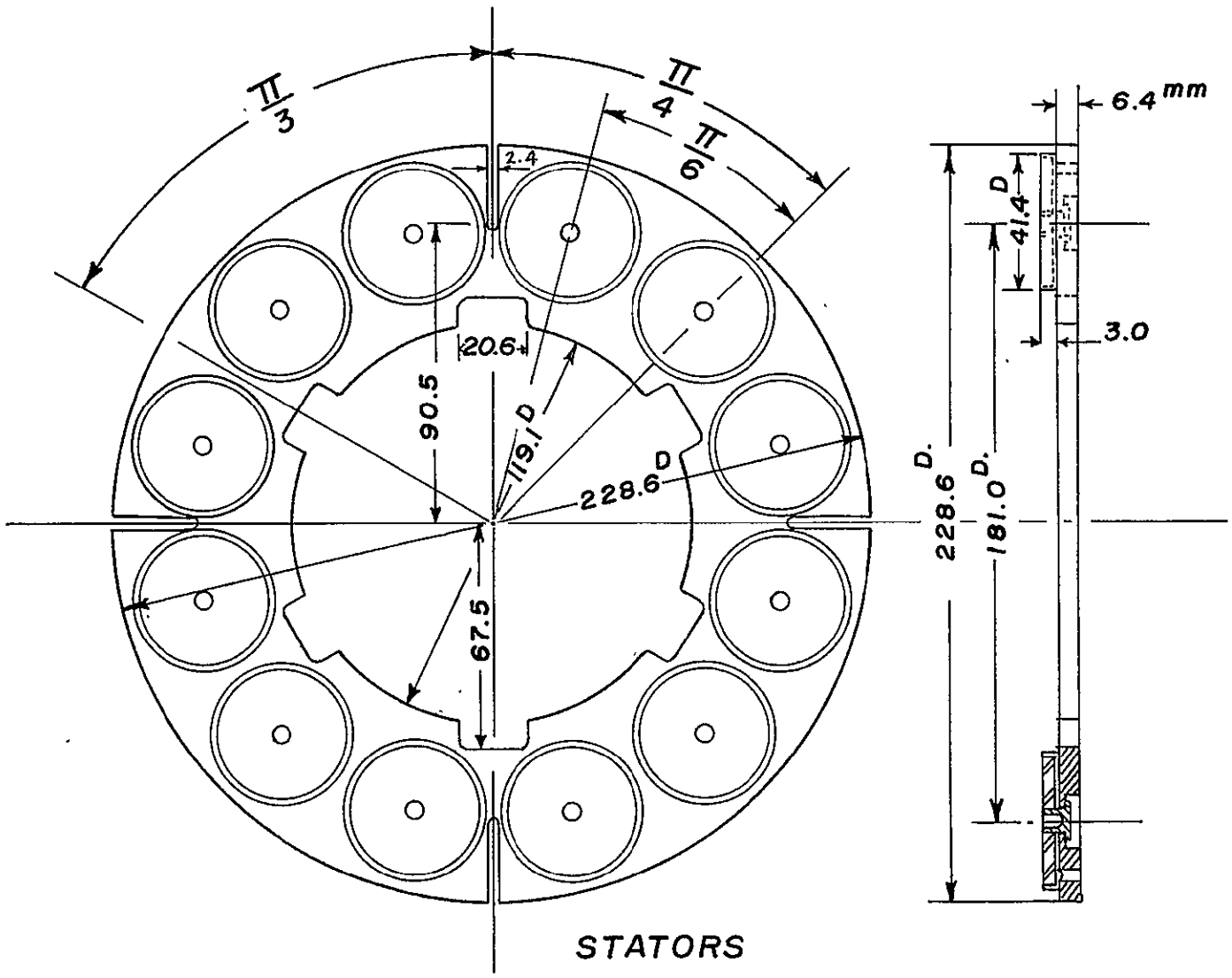

Figure 8 Diagram of Stator for Pad Brake

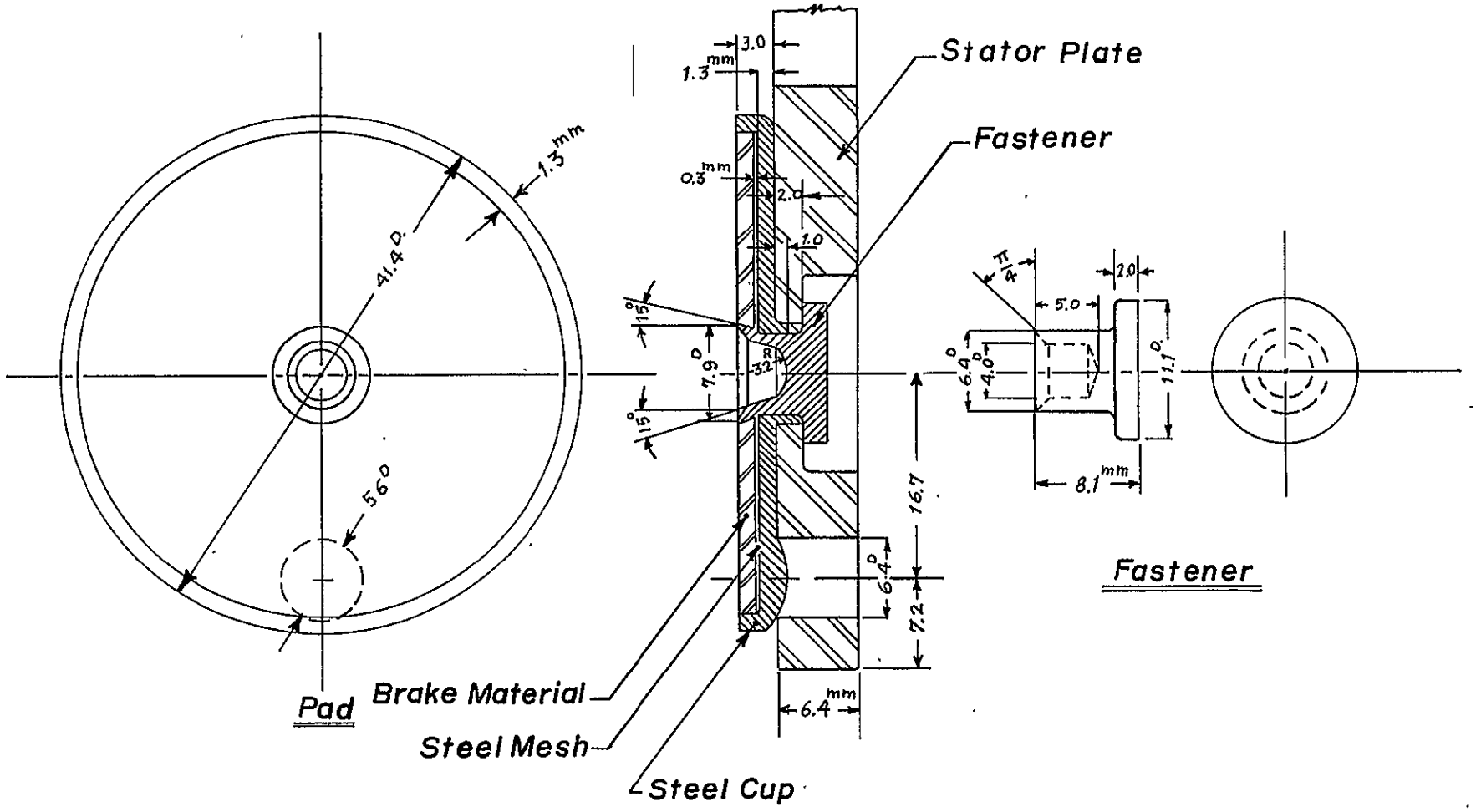

Figure 9 Assembly of Stator Friction Pads

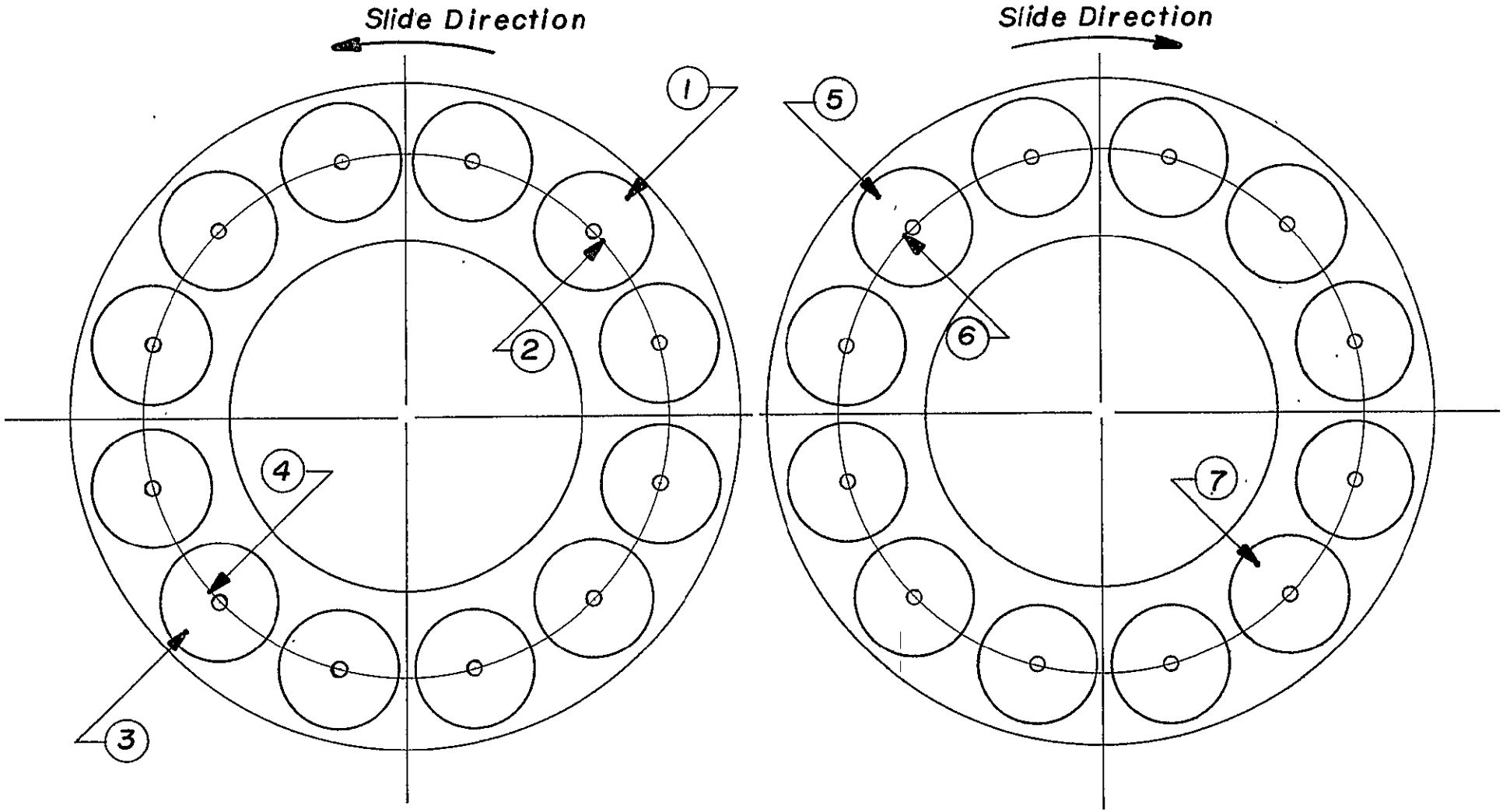

Figure 10 Location of Thermocouples in Pad Brake Stators

braking conditions, with a constant brake load being applied while the velocity decreased at a constant rate during the braking period. Other test series, run at constant velocity, were meant to provide different values of kinetic energy input to the brake during the braking runs. Low energy runs, such as series 6, simulated energy input during taxiing, while others simulated energy absorbed during a normal aircraft landing. The single rotor brake used in the experimental work had a rated capacity of 10^6 Joules in a normal landing.

TABLE 2

TEST CONDITIONS

Series Number	Load (N)	Rotational Speed		Braking Time (sec)	Number of Runs	Annular	Slotted	Button	Pad
		rad/sec	rpm						
1	3250	90	875	30	6	X	X	X	X
2	3250	180	1750	40	5	X	X		
3	3250	180	1750	30	5			X	X
4	3250	180 → 90	1750 ~ 875	30 (approx)	5	X	X	X	X
5	6500	90	875	20	5	X	X	X	X
6	6500	32		30	5	X	X	X	
7	6500	180	1750	20	5			X	X
8	6500	90 → 0	875 → 0	30 (approx)	5	X	X	X	
9	6500	180 → 0	1750 → 0	30 (approx)	5				X

5.2 Results and Discussion

Two separate sets of comparisons were made during the design evaluation phase of this work. First, three different brake configurations, each using copper-based friction material, were compared. The brakes were an annular brake

(Brake A), a slotted annulus brake (Brake B) and a pad brake (Brake E). Later, two different comparisons were made of button brakes vs. pad brakes, one using nickel-based friction material (Brakes C and F) and the other using molybdenum-based material (Brakes D and G),

5.2.1 Comparison between Annular, Slotted Annular, and Pad Brakes

During test runs on each brake, continuous measurements were made of frictional torque, brake load, rotating velocity, and temperature at seven different locations in the brake. From the temperature measurements, average brake surface temperatures were determined, and from the torque and velocity measurements, the kinetic energy absorbed by each brake was determined. Wear measurements were made by determining weight loss during braking. Basically, test series 1,3,5,7 (see Table 2) were employed for materials evaluation.

Wear. The wear recorded during tests on the three brakes is shown in Figure 11 as a function of kinetic energy input. It can be seen that at low energy levels, each of the three brake configurations yields approximately the same wear. The slotted annular brake (Brake B) may have slightly greater wear than the other two designs for low energy inputs, but the data is by no means conclusive. It is seen that at energy levels greater than that for a normal landing ($\approx 10^6$ Joules) the wear increases rapidly. The wear increase seems to be least for the full annulus, with the slotted annular brake and the pad brake being somewhat higher. This corresponds with the amount of sliding surface available for wear, with pad brake and slotted annular brake having 75% and 80%, respectively, as much friction material surface area as the annular brake (see Section 5.1). At such high energy levels the apparent contact area may affect the amount of wear.

It should be noted that as the energy input to the brake increases toward that which must be absorbed in a rejected take-off ($\approx 2.5 \times 10^6$ Joules), the wear increases tremendously. Wear in low-energy runs, such as taxiing, is nearly as great as that in moderate energy applications, such as landing stops.

Friction. A comparison was also made of the frictional performance of the three brake configurations. A typical comparison is shown in Figure 12, which shows the coefficient of friction as a function of time during a typical test run. The test conditions - brake pressure, rotating velocity (constant during test), and braking time - were the same for each of the three brakes, as was, within 1%, the kinetic energy input. As can be seen from the curves, the coefficient of

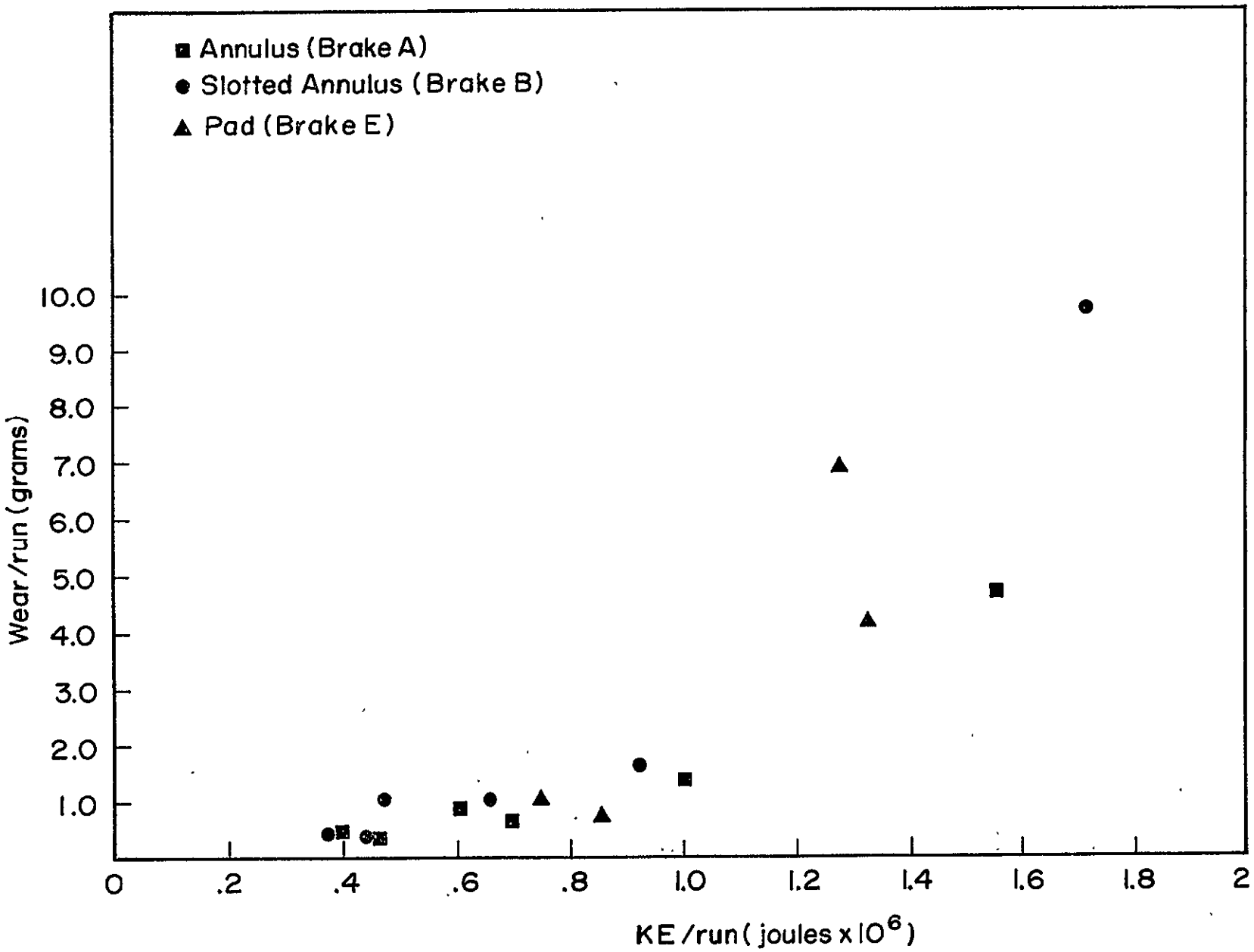

Figure 11 Effect of Absorbed Kinetic Energy on Wear for Brakes A. B, and E

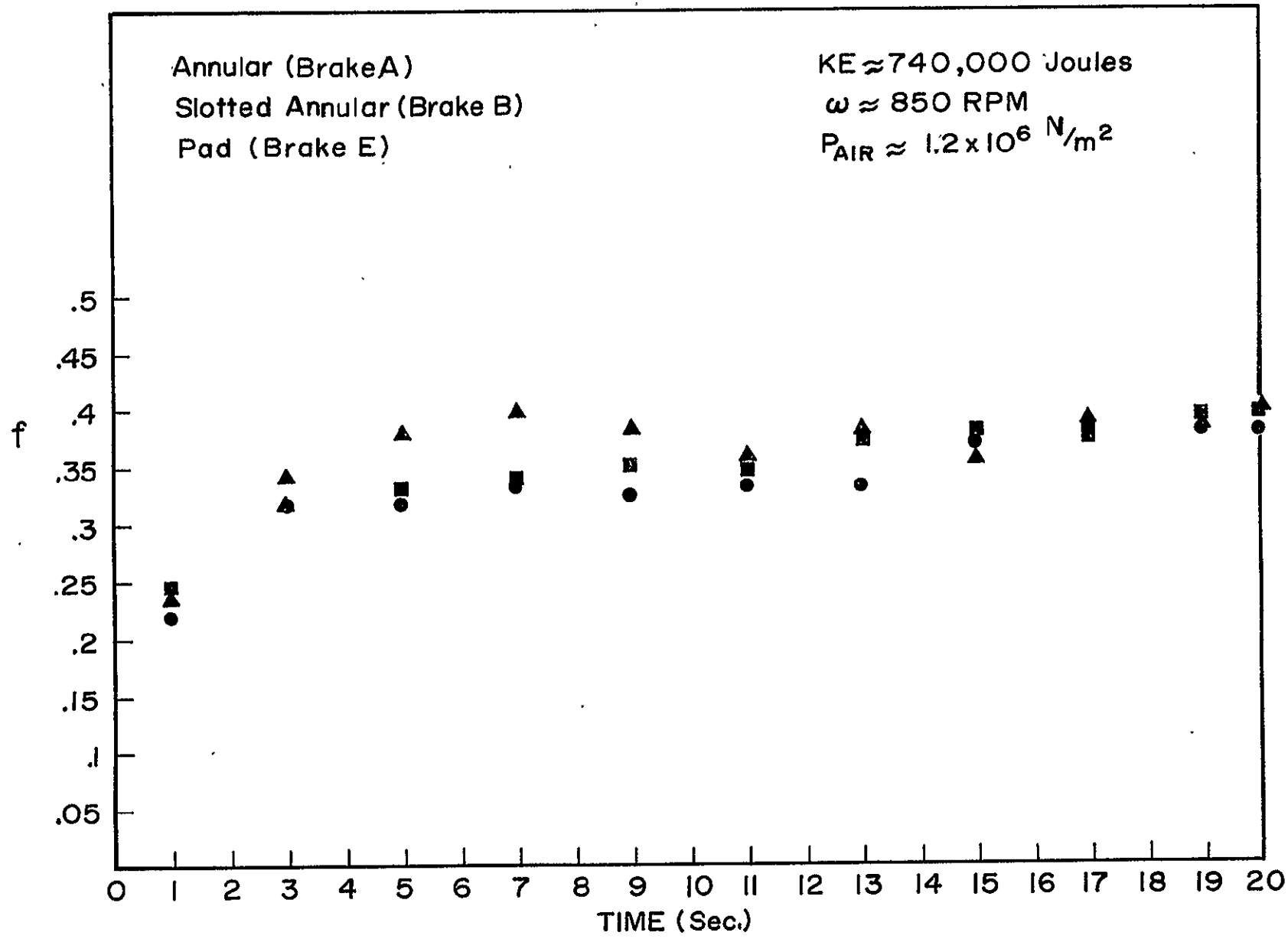

Figure 12 Typical Variation of Friction Coefficient with Time for Brakes A, B, and E

friction was nearly the same for all three brake configurations. The friction coefficient for pad brake rose more rapidly than for the other designs, but all leveled off to approximately the same value. As the figure shows, the friction coefficient remained relatively constant during most of the test run. The variations in friction coefficient that did occur can be traced to two causes: the effect of temperature on friction and the effect of velocity on friction. Both of these effects are primarily a function of the sliding materials and will be discussed in Section 6 of this report. Briefly, it was found that, for all three brake designs using copper-based friction material, the coefficient of friction increased gradually with increasing surface temperature until reaching a maximum at about 450°C and then decreased as the temperature approached the melting point. The friction coefficient decreased slightly with increasing velocity for all three brake configurations, but the decrease was less for the copper-based material than for other materials. These effects will be discussed in greater detail later.

In summation, the comparative evaluation of the annular, slotted annular, and pad brakes showed relatively minor differences between the three. Although the slots on the annular brake did not adversely affect surface temperatures, the wear was greater, especially at high energy levels. The pad brake also had greater wear than the annular brake at high energy levels, but showed advantageous friction performance. There were some indications that wear at high energy levels is affected by the nominal contact area of the friction material component, with greater wear occurring with smaller area.

5.2.2 Comparison between Button and Pad Brakes

A study of friction and wear behavior was carried out for four brakes labeled C, D, F, and G (Table 1) with different friction materials sliding against 1722 AS steel under a variety of test conditions as described in Table 2. The advantage of the button configuration is the reduction in apparent contact area up to 41% and the weight of stator around 43% for nickel-based material or 32% for Mo/LPA material in comparison with those of the pad brake. The results are discussed as follows.

Wear. As shown in Figure 13, the total wear per run is plotted versus the kinetic energy absorbed by the brake during the run. At low energy levels (less than 5×10^5 Joules) there is no significant difference in wear between the brakes.

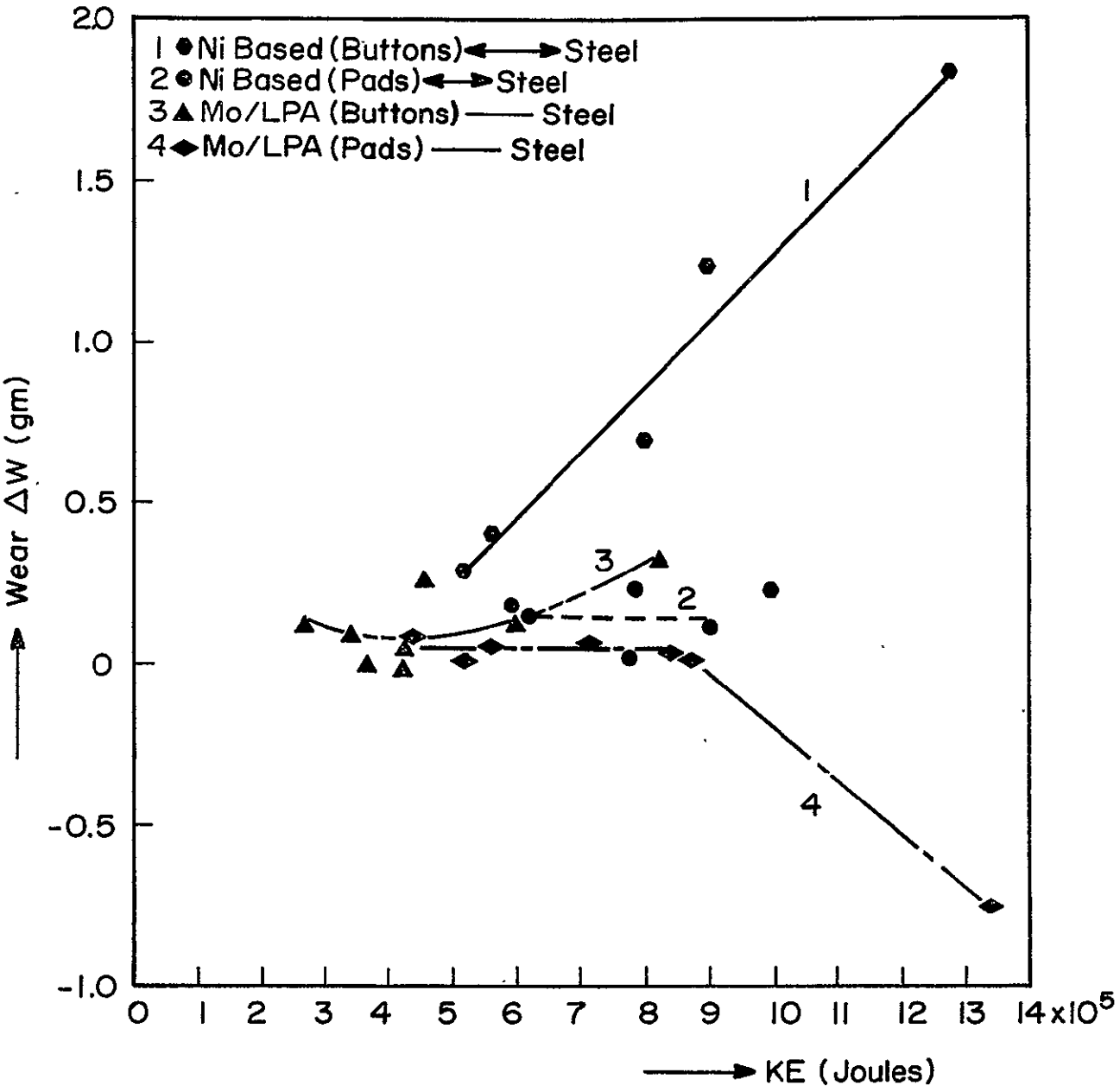

Figure 13 Effect of Absorbed Kinetic Energy on Wear for Brakes C, D, F, and G

The wear is not greater than 0.3 gm per run. The pad brakes give constant wear up to the high-energy region except that one point of the brake G has negative value. This happens because of material transfers from heat-softened steel disk to the brake pads. However, the button brakes yield increasing wear behavior in the high-energy range. It is seen that the increase is slight for the button brake D with Mo/LPA material but it is linear for the button brake C with nickel-based material.

Similar curves are shown in Figure 14 where the wear is plotted versus the average surface temperature measured in brake material near the sliding interface. It is felt that the steel jacket used with the pads is important to support the brake material which is usually porous and fragile. The nickel-based material with a high percentage of graphite has soft and easily sheared off edges. This results in the significant increase in wear for the button brake C compared with the data of the pad brake F. The Mo/LPA material is stronger so it is less susceptible to edge cracking.

Friction. In Figure 14, a comparison of the friction-temperature performance is also shown for the four brakes (Brakes C, D, F, and G). It is seen that brakes D and G have approximately the same friction-temperature relation. The friction coefficient drops from 0.3 to 0.1 when the temperature increases from 200 to 300°C, then it stays level at 0.1 up to 600°C (Curves 5 and 7). However, the friction-temperature curve for brake C (Curve 1) decreases gradually from 0.6 to 0.25 as the temperature increases from 250 to 700°C. It stays quite higher than that for brake F (Curve 3) which shows the drop of friction coefficient from 0.3 to 0.14 at temperatures of 520°C. It is felt that the oxide film is more easily removed on the sliding surface of the button configuration. It is the way in which the metal contact sill dominates the sliding of brake C at higher temperatures and results in high friction and high wear.

In Figure 15, two photographs show the rubbed surface conditions of the stators, one with Mo/LPA buttons and the other with nickel-based buttons, at the conclusion of all evaluation tests. There is a lot of damage at the rear edges of the nickel-based buttons due to the low strength of the nickel-based material. It is seen that it did not happen for the Mo/LPA buttons.

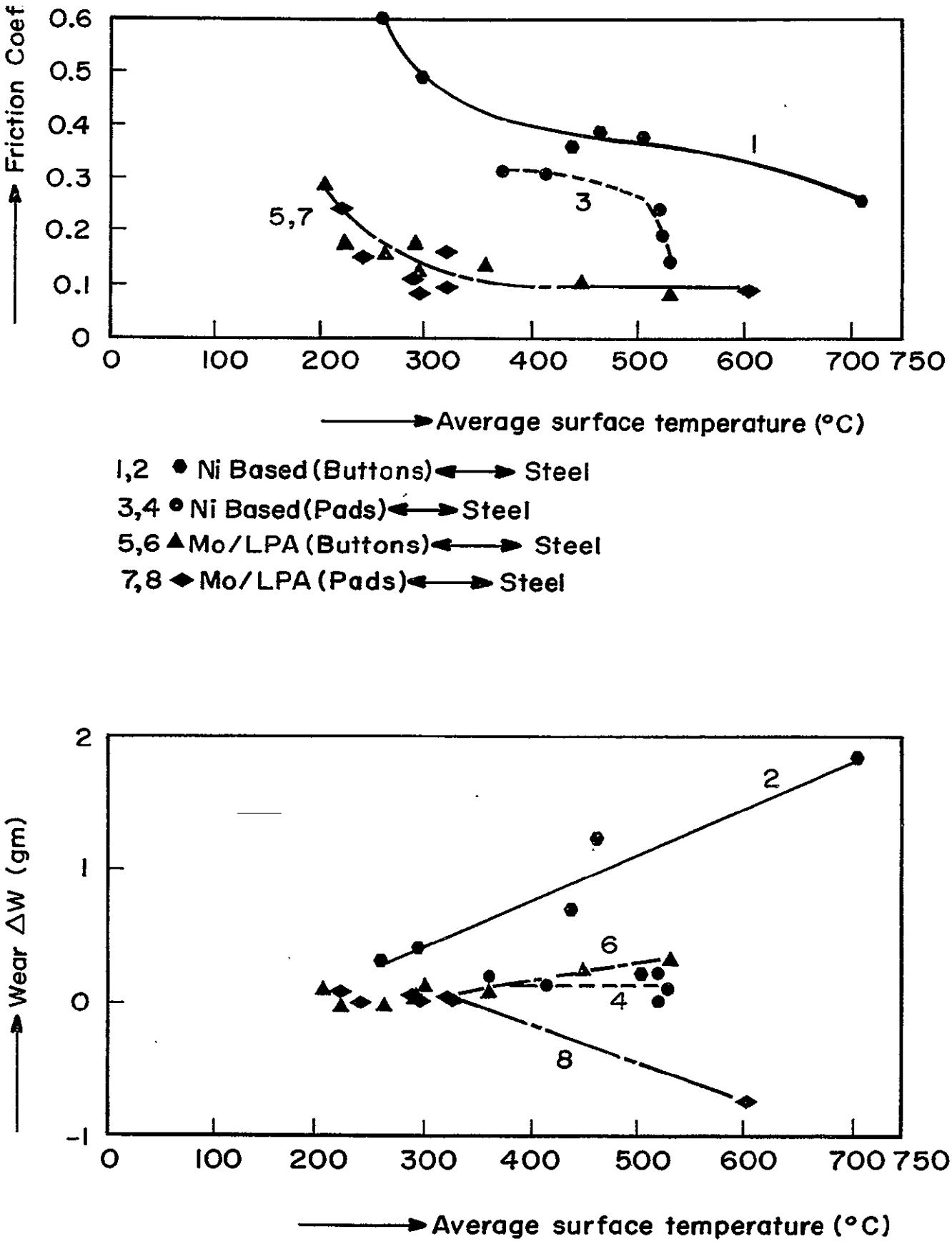

Figure 14 Effect of Average Surface Temperature on Friction and Wear for Brakes C, D, F, and G

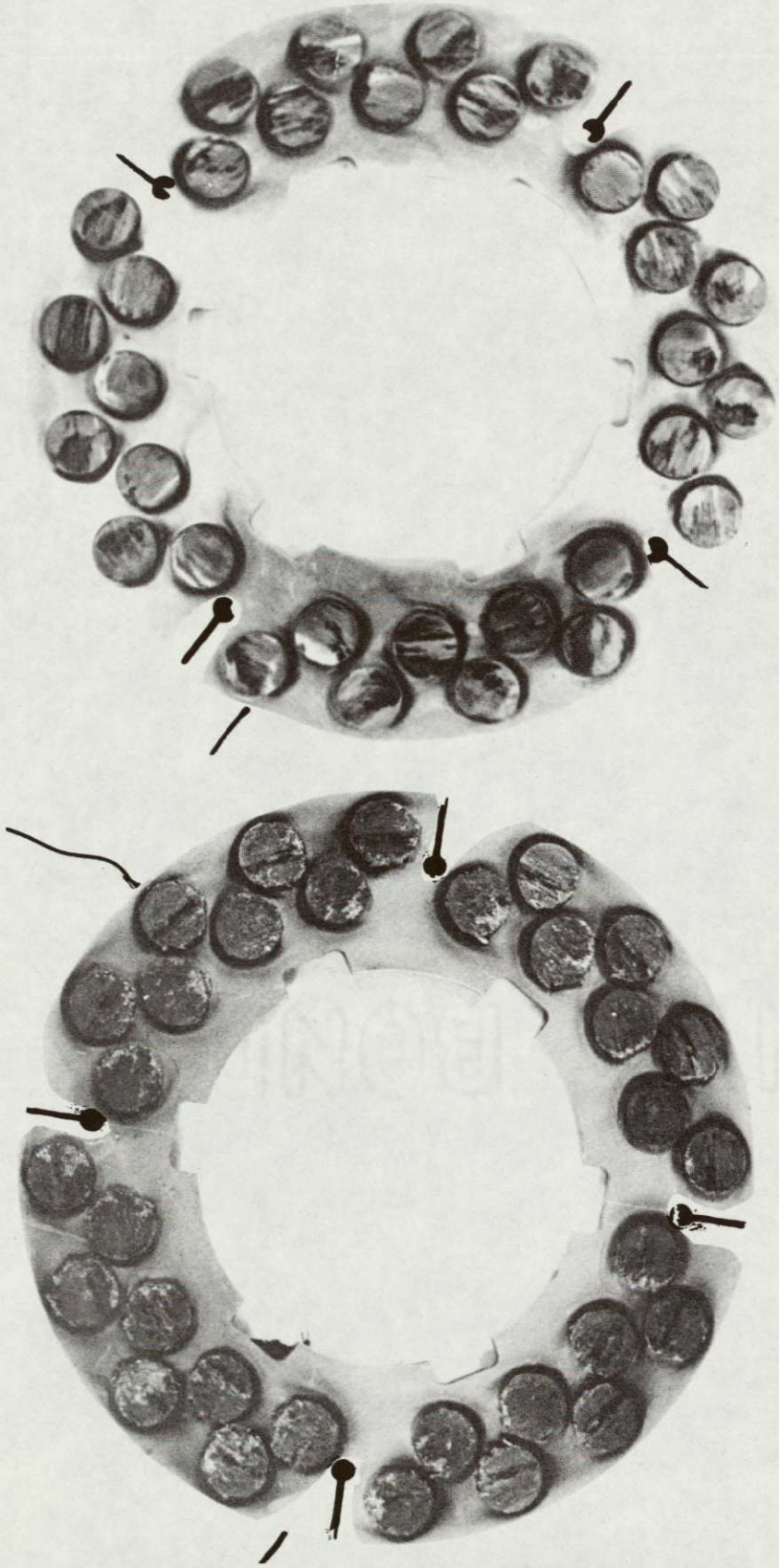

Figure 15 Photographs Showing the Rubbed Surface Conditions of Stators, One with Mo/LPA Buttons and the Other with Nickel-Based Buttons after all Evaluation Tests

In summation, the button brake concept can be employed only for the brake material with high strength, especially at higher temperatures. Usually the button design gave higher wear than the pad brake. It is felt that the steel backing is needed to protect the edge from being worn away easily and to help the oxide film stabilizing on the sliding surface.

SECTION 6

EVALUATION OF BRAKE MATERIALS

6.1 Materials

Four kinds of new brake materials were made up in round pads for final evaluation in the actual brake test system. Table 3 lists a comparison of their chemical composition with volume percentage. The copper base brake pads and the carbon pads were obtained from commercial sources. The others were developed at RPI and manufactured into pads using the following processes:

1. Mixing. All chemical components were weighed according to the percentages and blended for 4 to 5 hours in a mixer to obtain a homogeneous mixture.
2. Compacting. The mixture was compacted into a steel cup under a pressure of 5.3×10^3 kg/cm^2. The green density is 6.89 gm/cm^3 for Mo/LPA 100, while 5.23 gm/cm^3 for nickel-based brake material.
3. Sintering. The sintering temperature and the sintering time depend upon the type of material. The nickel-based specimens were sintered at 1010°C for 2 hours and Mo/LPA 100 at 1220°C for one-half hour. Both kinds of specimens were sintered in vacuum furnace and cooled in N_2 to avoid the oxidation.
4. Coining. A range of pressure from 7.0 to 8.8×10^3 kg/cm^2 was employed to coin the pads and crimp the steel cup.
5. Finishing. The final step is grinding the pad surface in order to have a level frictional plane.

The photomicrographs in Figure 16 illustrate the surface conditions of the steel and four lining materials before the evaluation test.

1722 AS Steel

Cu-Based

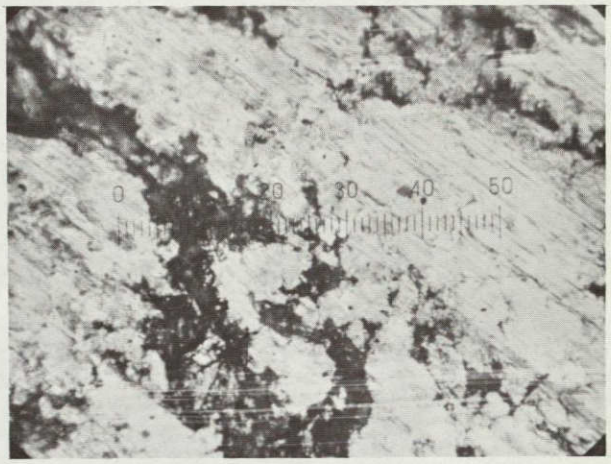

Ni-Based

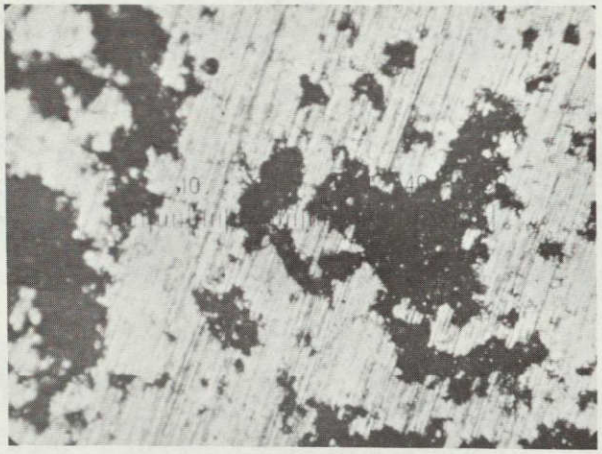

Mo/LPA 100

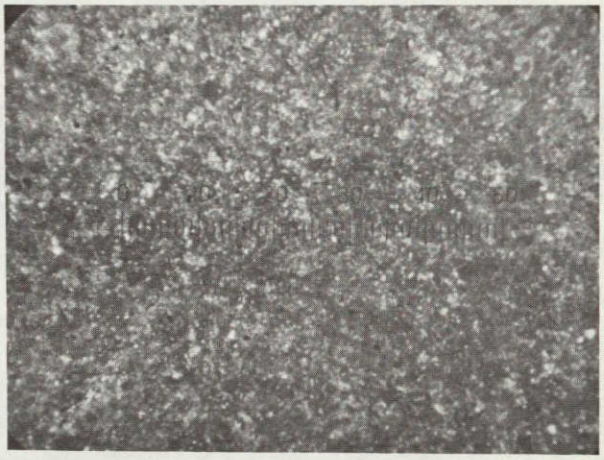

Carbon

Figure 16 Typical Photomicrographs (50 ×) Showing the Surface Conditions of the Steel and Four Lining Materials before the Testing

TABLE 3

CHEMICAL COMPOSITION OF FRICTION PADS

Function	Base Material	Lubricant	Abrasive	Friction Modifiers
Copper-based	Cu (31.0%)	Graphite (32.0%)	Mullite (22.0%)	(15.0%)
Nickel-based	Ni (47.6%)	Graphite (27.5%)	Al_2O_3 (19.8%)	$PbWO_4$ (5.0%)
Mo/LPA 100	Mo (50.0%)	-	-	LPA 100 (50.0%)
Carbon	P5	-	-	-

6.2 Test Conditions

A set of two stators with the pad configuration sandwiching a 1722 AS steel rotor disk was applied in this material evaluation program. The disk rotor was surface-finished and cleaned under the usual conditions as before. Then it and two stators were weighed and assembled in the brake. The whole rig is always well aligned before running to avoid any vibrational damage.

Each brake material was evaluated under several running series of different braking conditions by varying applied load, changing velocity, or increasing slide time. Basically, four running series were applied at first as follows:

1. Low load (3.24×10^3N), low speed (850 rpm) for 30 sec
2. Low load (3.24×10^3N), high speed (1700 rpm) for 30 sec
3. High load (6.31×10^3N), low speed (850 rpm) for 20 sec
4. High load (6.31×10^3N), high speed (1700 rpm) for 20 sec.

One more test series (load = 9.01×10^3N, speed = 1700 rpm, and time = 20 sec) was run for the nickel-based material, while three more for Mo/LPA 100 as follows:

1. Load = 9.01×10^3N, speed = 1700 rpm, and time = 30 sec
2. Load = 10.81×10^3N, speed = 1700 rpm, and time = 30 sec
3. Load = 12.61×10^3N, speed = 1700 rpm, and time = 40 sec

in order to get the data up to higher energy levels. Each test series consisted of five engagements each started from the room temperature condition. All data reported are the average values of each test series.

In this study the effect of variation of rotor velocity on the frictional behavior of the brake materials was considered. This is important from a safety point of view. Frictional vibration in the brake can cause structural damage in the landing gear as well as brake "squeal."

In order to determine the effect of the rotational speed of the wheel on the frictional coefficient, two more kinds of tests were run under both conditions of so-called "low load" and "high load" as described before. First the braking is applied with full speed (1700 rpm) for 5 sec to get a steady-state situation, the power source of electric motor is then turned off. The braking continues through the whole velocity range to a dead stop. The second kind of test is run exactly the same at the beginning (5 sec, steady state), then the braking proceeds for 25 sec with the velocity decreasing from the maximum value to zero.

In addition a microscopical inspection of the rubbing surface was made for both the lining material and steel disk. Also in conjunction with this research, another project is underway to determine the fundamental theory of wear mechanism in high energy braking systems.

6.3 Results and Discussion

A summary of the results is listed in Table 4 for the copper-based material, Table 5 the nickel-based material, Table 6 Mo/LPA 100 and Table 7 the carbon material. The international system of units was applied in the representation. The first three items are the external variables of the test; the others, the results measured at the end of the braking. The results are discussed as follows:

6.3.1 Effect of Frictional Energy on Wear

The average frictional energy of braking is determined as follows: At the end of each two-second period of braking, angular velocity (V_i) and frictional torque (q_i) were measured, where i is the index of time period of two seconds. Their product gives the instantaneous frictional power at that particular time.

TABLE 4

EVALUATION TEST SERIES FOR
A COPPER-BASE BRAKE MATERIAL

Test Series		1	2	3	4
Apparent Pressure of Contact (N/m^2)		2.31×10^5	2.29×10^5	4.12×10^5	4.07×10^5
Angular Velocity of Wheel (rpm)		850	1680	840	1680
Braking Time (sec)		30	30	20	20
Friction Coefficient $(f)_{end}$		0.43	0.30	0.39	0.21
Local Surface Temperature at End of Braking (C)	T_1	493	664	528	753
	T_2	442	699	457	826
	T_3	508	686	544	644
	T_4	407	621	381	707
	T_5	419	683	451	625
	T_6	340	550	404	573
	T_7	318	503	278	515
Average Surface Temperature (C)		418	629	435	663
Frictional Kinetic Energy, KE (Joules)		8.57×10^5	13.25×10^5	7.51×10^5	12.74×10^5
PV (N/m^2) (rad/sec)		2.06×10^7	4.07×10^7	3.61×10^7	7.16×10^7
Stators	Total Wear (gm)	0.68	4.19	0.98	6.90
	Wear Rate (gm/s)	0.023	0.140	0.049	0.345
Rotor	Total Wear (gm)	0.025	2.280	0.326	1.558
	Wear Rate (gm/s)	0.001	0.076	0.016	0.078

TABLE 5

EVALUATION TEST SERIES FOR
A NICKEL-BASE BRAKE MATERIAL

Test Series		1	2	3	4	5
Apparent Pressure of Contact (10^5 N/m^2)		2.20	2.17	4.00	4.00	5.78
Angular Velocity of Wheel (rpm)		870	1690	870	1670	1660
Braking Time (sec)		30	30	20	20	20
Friction Coefficient $(f)_{end}$		0.31	0.24	0.31	0.19	0.14
Local Surface Temperature at End of Braking (C)	T_1	440	521	383	552	553
	T_2	394	608	528	507	479
	T_3	234	319	222	476	667
	T_4	354	626	529	547	469
	T_5	410	522	479	686	584
	T_6	436	604	517	522	438
	T_7	243	302	240	350	507
Average Surface Temperature (C)		359	521	414	523	528
Frictional Kinetic Energy (10^5 Joules)		5.92	7.84	6.13	7.78	9.00
PV (10^7 N/m^2)(rad/sec)		1.96	3.85	3.66	6.97	10.10
Stators	Total Wear (gm)	0.18	0.23	0.14	0.02	0.11
	Wear Rate (gm/sec)	0.006	0.008	0.007	0.001	0.006
Rotors	Total Wear (gm)	0.15	0.02	0.08	0.34	0.86
	Wear Rate (gm/sec)	0.005	0.001	0.004	0.017	0.043

TABLE 6

EVALUATION TEST SERIES
FOR Mo/LPA100 MATERIAL

Test Series		1	2	3	4	5	6	7
Apparent Pressure of Contact (10^5 N/m^2)		2.01	2.01	4.07	4.14	5.78	6.93	8.09
Angular Velocity of Wheel (rpm)		850	1680	850	1670	1670	1670	1650
Braking Time (sec)		30	30	30	30	30	30	40
Friction Coefficient $(f)_{end}$		0.24	0.16	0.15	0.11	0.09	0.08	0.09
Local Surface Temperature at End of Braking (C)	T_1	271	341	280	324	408	433	667
	T_2	288	302	300	391	386	202	721
	T_3	211	275	-	264	330	-	557
	T_4	234	431	229	227	263	157	626
	T_5	221	257	206	238	279	324	584
	T_6	168	241	164	224	180	202	522
	T_7	159	203	257	341	417	454	554
Average Surface Temperature (C) ——		220	321	239	287	323	295	605
Frictional Kinetic Energy (10^5 Joules)		4.38	5.59	5.18	7.12	8.40	8.70	13.36
PV (10^7 N/m^2)(rad/sec)		1.85	3.56	3.64	7.28	10.10	12.20	13.99
Stator	Total Wear (gm)	0.084	0.054	0.004	0.068	0.040	0.010	-0.75
	Wear Rate (gm/sec)	0.003	0.002	10^{-4}	0.002	0.001	3×10^{-4}	-0.019
Rotor	Total Wear (gm)	0.088	0.086	0.050	0.270	0.590	0.620	1.510
	Wear Rate (gm/sec)	0.003	0.003	0.002	0.009	0.020	0.021	0.038

TABLE 7

EVALUATION TEST SERIES FOR CARBON

Test Series		1	2	3	4	5	6	7
Apparent Surface Pressure of Contact (N/m^2)		2.20×10^5	2.21×10^5	4.25×10^5	4.32×10^5			
Angular Velocity (rpm)		860	1650	840	1640			
Braking Time (sec)		30	30	20	20			
Friction Coefficient $(f)_{end}$		0.19	0.32	0.30	0.23			
Local Surface Temperature at End of Braking (°C)	θ_1	120	588	181	230			
	θ_2	375	806	161	666			
	θ_3	142	418	202	410			
	θ_4	113	264	409	481			
	θ_5	170	690	274	690			
	θ_6	275	514	396	711			
	θ_7	74	358	238	790			
Average Surface Temperature (°C)		192	571	300	568			
Frictional Kinetic Energy (KE) (Joules)		2.68×10^5	8.96×10^5	5.32×10^5	10.60×10^5			
PV (N/m^2)(rad/sec)		1.98×10^7	3.83×10^7	3.78×10^7	7.42×10^7			
Stators	Total Wear (gm)	0.60	1.61	0.62	3.27			
	Wear Rate (gm/sec)	0.020	0.054	0.031	0.164			
Rotor	Total Wear (gm)	0	0.70	1.02	4.30			
	Wear Rate (gm/sec)	0	0.023	0.051	0.215			

An approximation was then employed to gain the total frictional energy (KE) of each test by adding up all products of the time of two seconds and this instantaneous power at the end of each two second period during the whole brake application:

$$KE = \sum_{i=1}^{n} (2)\ V_i q_i = 2 \sum_{i=1}^{n} V_i q_i$$

where n is the total number of time periods in a braking test. The average value of five tests in each test series for this accumulated energy was plotted against the wear (which is one-fifth of the difference between weights measured before and after that test series) in Figure 17 for the brake materials. Curve 1 shows the wear of the conventional brake material in the high-energy range.
Curves 2 and 3 show the data for the nickel-based material and Mo/LPA 100, respectively. These developmental materials showed low wear at all energy levels. One point for the Mo/LPA 100 results in an extremely high energy range, shows that the material gains weight. This happens because of material transfer from heat-softened steel near the inner radius portion of rotor disk to the brake pads. This phenomenon will be discussed in later surface investigation section. The wear-energy behavior of carbon material is shown as Curve 4. It has three times the wear of the nickel-based or Mo/LPA 100 materials. Around the energy range of the normal landing ($\approx 10^6$ Joules) the wear increases rapidly with the same magnitude as the current copper-based material. Therefore, as far as the wear-energy behavior is concerned, the brake materials with the greatest potential are the nickel-based material and Mo/LPA 100.

Similarly, the wear of steel disk rotor per run was plotted versus the frictional kinetic energy accumulated during the run as shown in Figure 18. Only one curve (1) is found for the wear-energy behavior of steel disk rubbed against the first three materials (copper-based, nickel-based and Mo/LPA 100). This means that there is no effect of these three lining materials on the wear of their mating steel. Another curve (2) shows the wear of steel rubbed against carbon.

Because of the low thermal conductivity with the carbon materials a greater proportion of the generated heat is directed into the rotor. The increase in temperature of the rotor could result in higher wear rates.

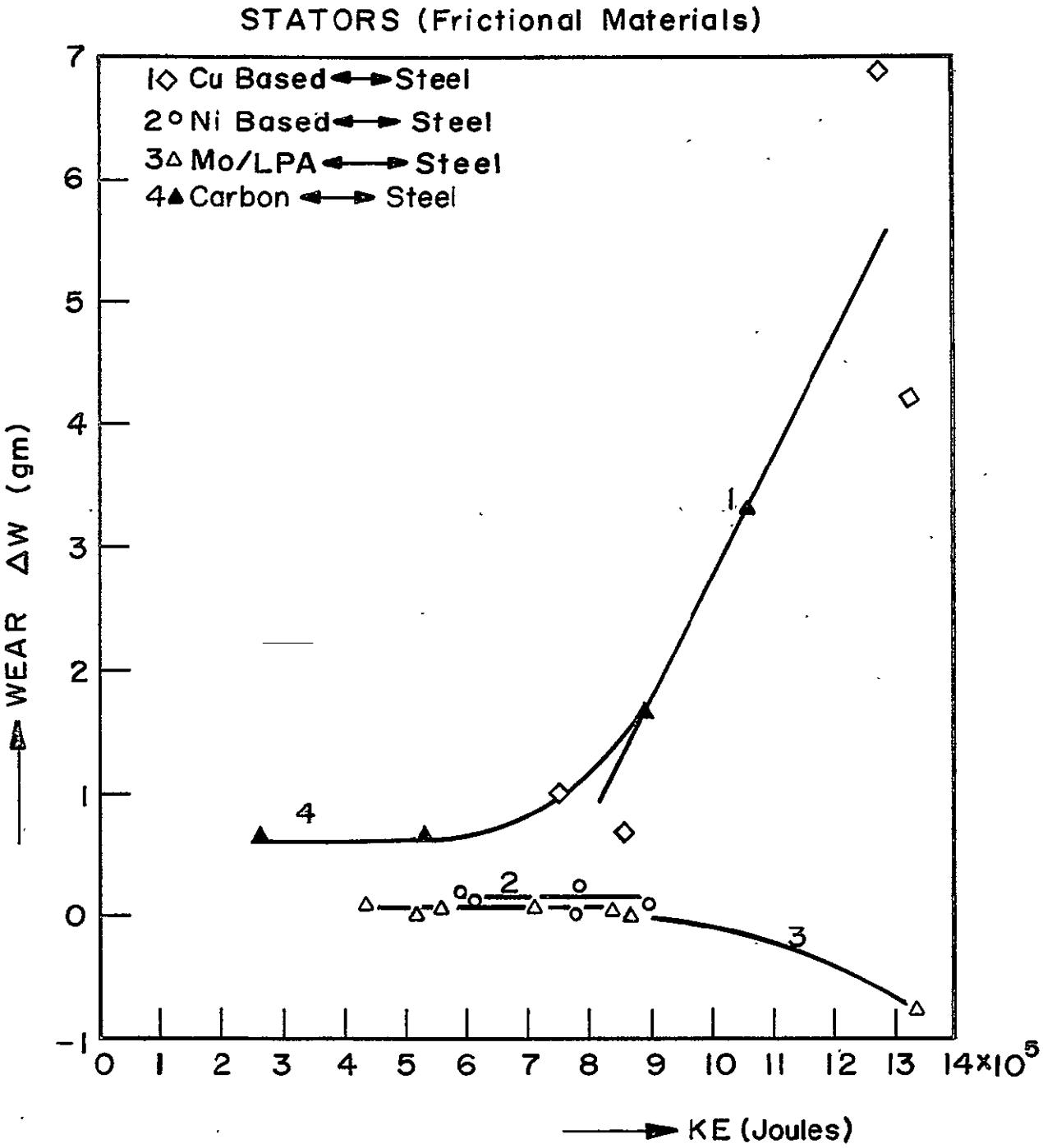

Figure 17 The Effect of Total Frictional Kinetic Energy on Wear of the Friction Materials

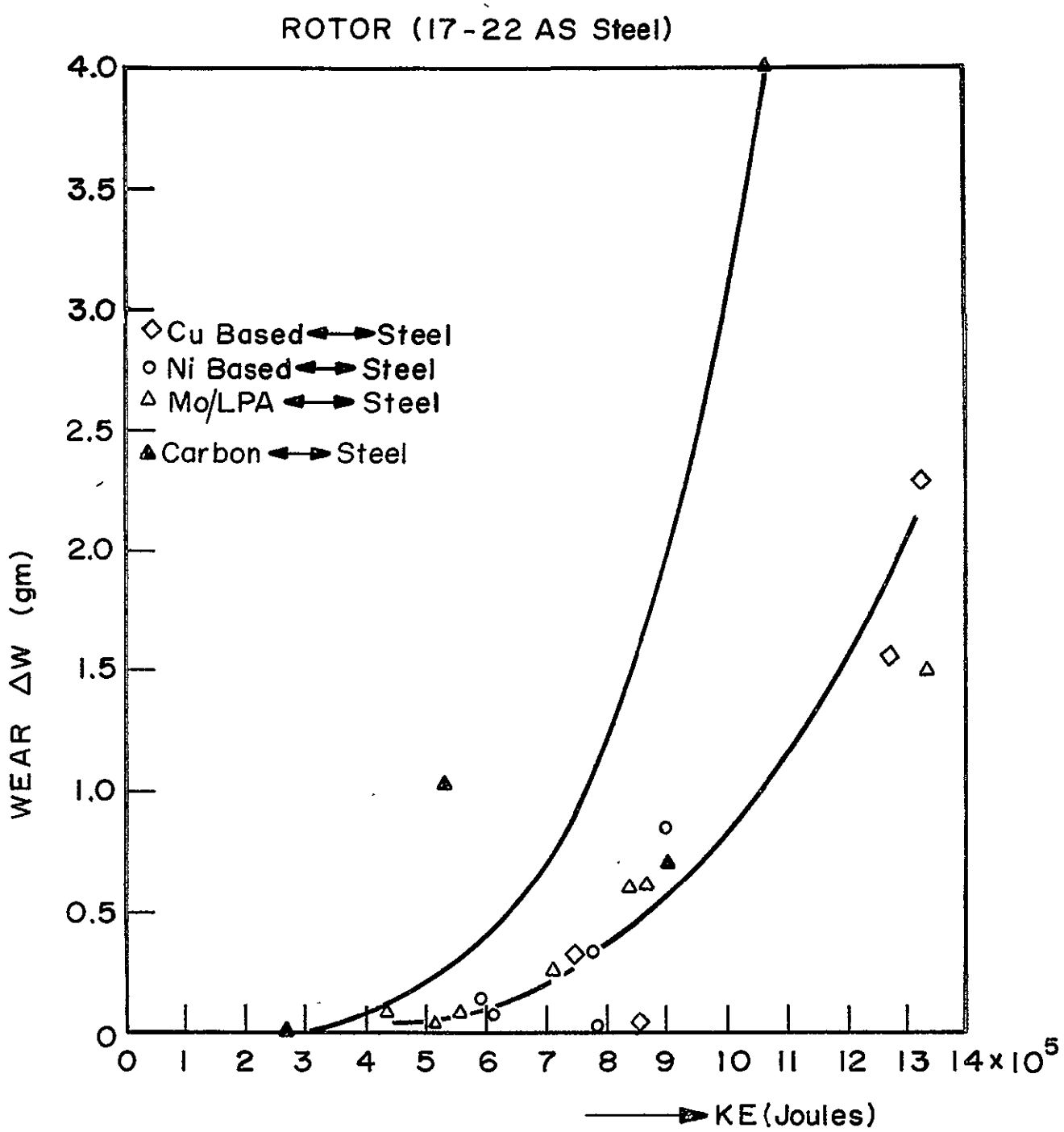

Figure 18 The Effect of Total Frictional Kinetic Energy on the Wear of Steel Disk

Furthermore, both curves indicate the high wear of the steel disk at high energy levels. Therefore some improvement on the high temperature strength of steel should be made or higher temperature materials should be utilized.

6.3.2 Effect of PV on Wear Rate

The apparent surface pressure of contact is P and V is the angular speed of the wheel. The product of them indicates the external loading power of the brake system. What the engaging capacity of the rubbing material is, can be shown by the relation between the wear rate and this PV factor.

The PV factor of each test is the average value of the instantaneous PV factors measured at the end of each two second period during braking. The average value of each test series was then plotted against the wear rate of the lining materials in Figure 19, and against that of the steel disk in Figure 20.

In Figure 19, Curves 1 and 4 show that the conventional brake material and carbon, respectively, have high wear rates at low PV. However, the other two developmental brake materials were found to be excellent contact materials for sliding against a steel disk, as shown in Curve 2 for nickel-based material and Curve 3 for Mo/LPA 100. They remain near zero for PV values up to 14×10^7 N/m^2-sec.

Figure 20 shows the steel disk has lowest wear rate curve (3) when it slides against Mo/LPA 100. Curve 4 shows that the worst condition for the wear rate-PV behavior is against carbon. It should be noted that the wear of the steel rotor generally follows the thermal conductivity of the brake material. When more heat flows into the brake material the wear of the steel is lowered significantly.

6.3.3 Effect of Temperature on Friction and Wear

The local surface temperatures listed in the last four tables were obtained by the measurement of seven thermocouples near the sliding surface in lining materials. The installation position of these thermocouples was arranged as shown in Figure 10.

Both friction-temperature and wear-temperature behaviors for the brake materials are shown in Figure 21. The frictional coefficient which is of the

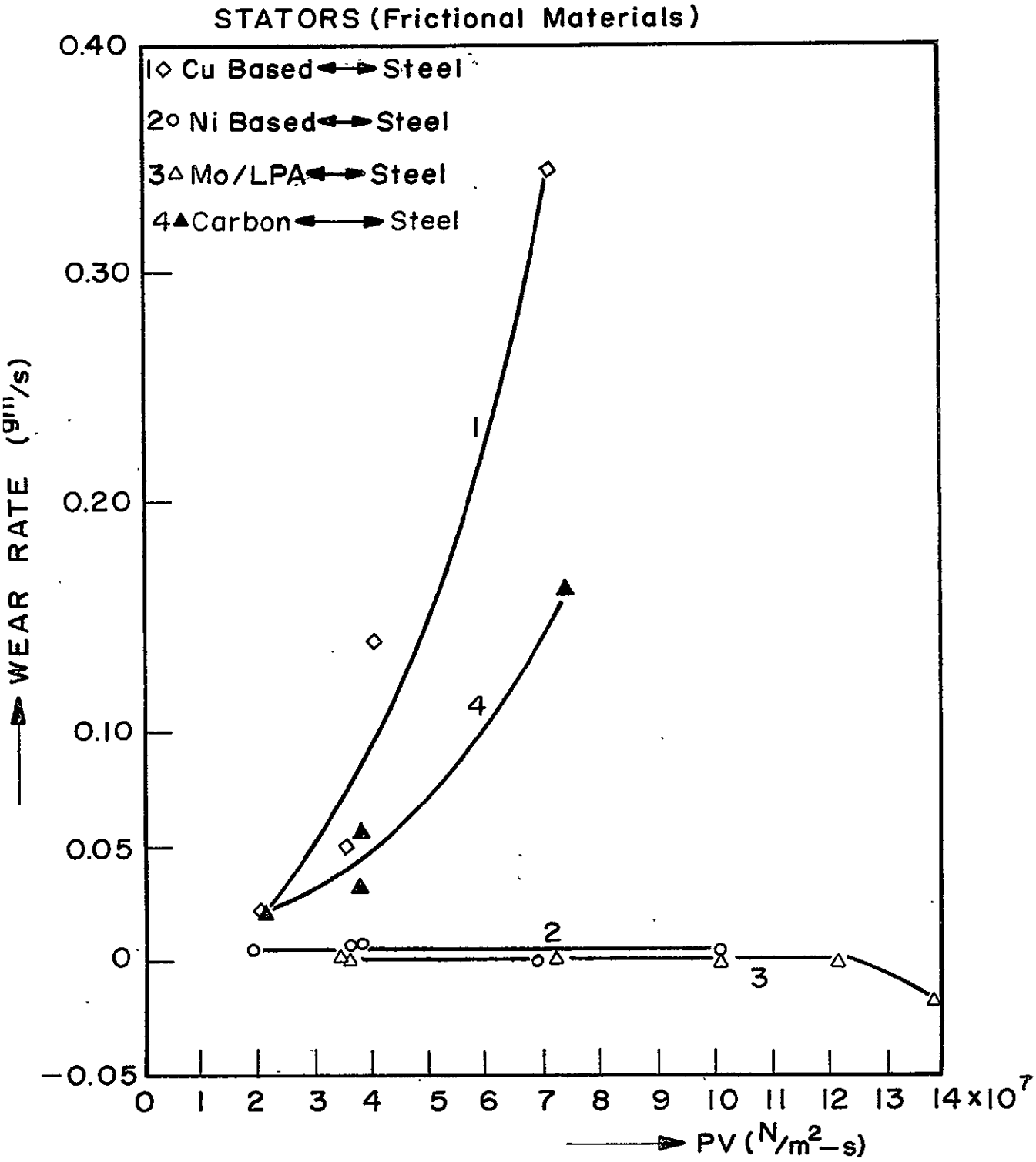

Figure 19 The Effect of PV Factor on the Wear Rate of Friction Materials

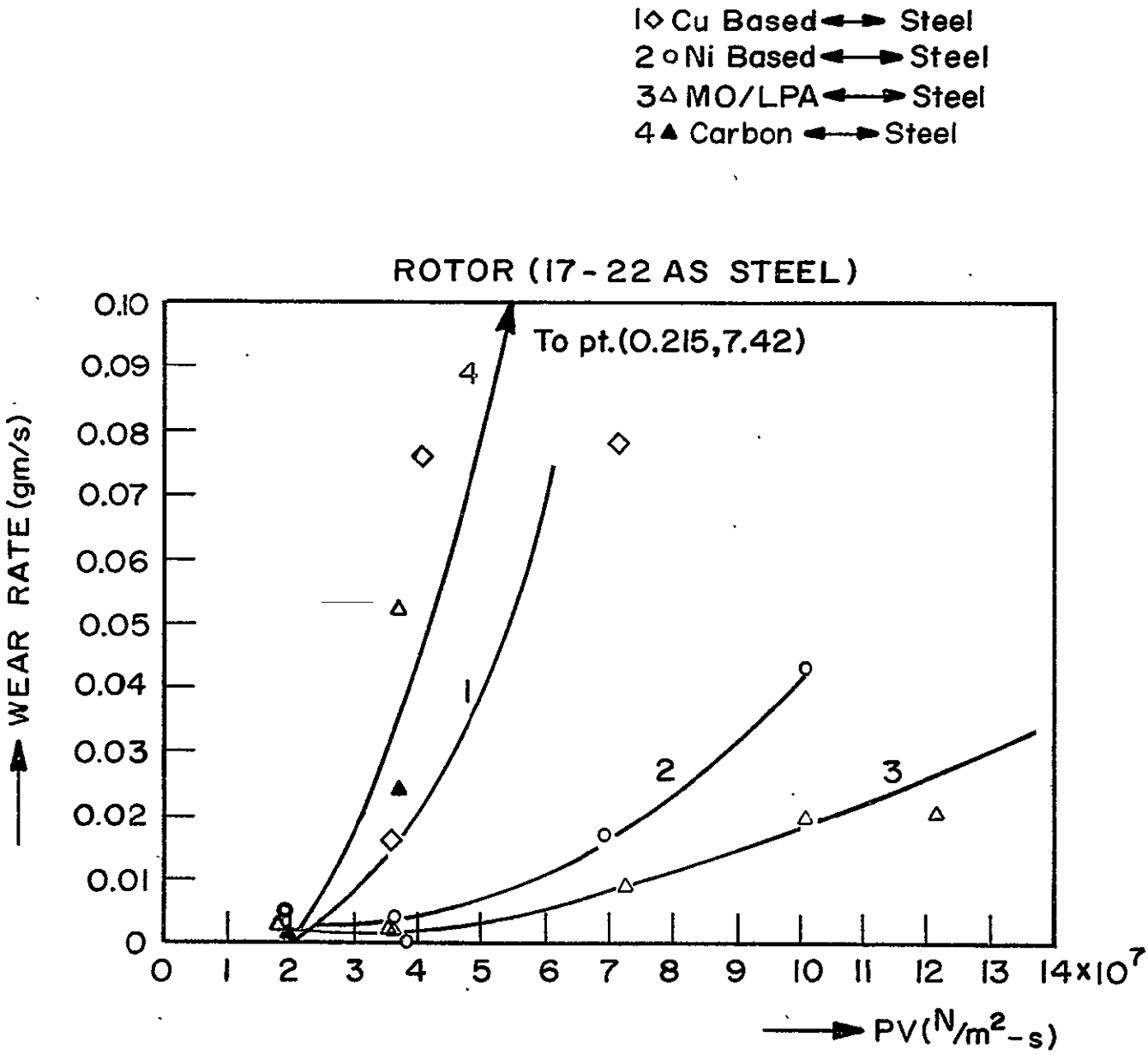

Figure 20 The Effect of PV Factor on the Wear Rate of Steel Disk

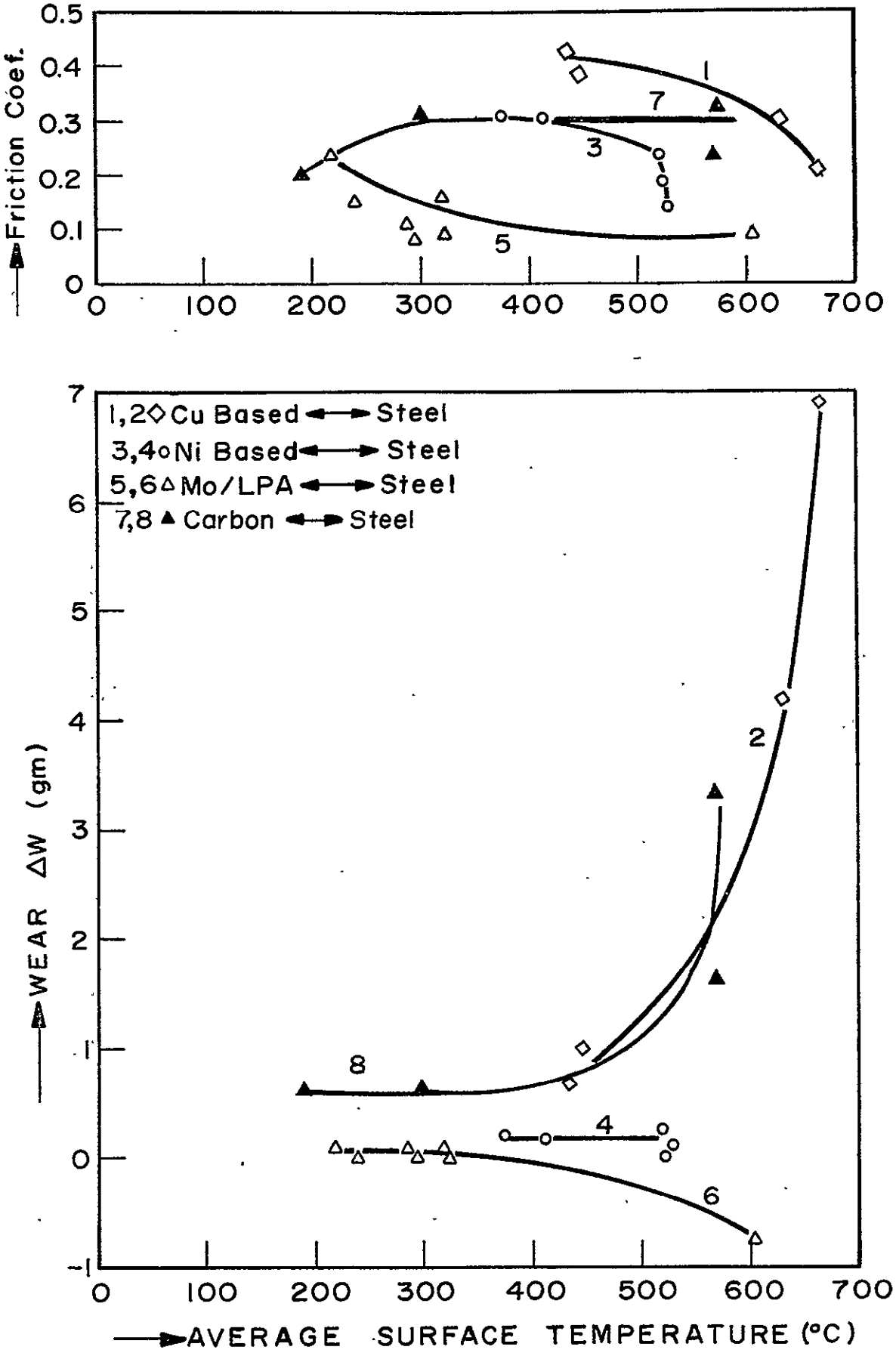

Figure 21 The Effect of the Average Surface Temperature on the Wear and Friction Behavior of Brake Materials

order of 0.4 at temperature of 450°C drops to 0.3 at 630°C and finally to 0.2 at 660°C for the conventional brake material. The total wear of this brake material increases abruptly from 1 gm at 450°C to 4 gm at 630°C and finally to 7 gm at 660°C. Evidently the drop of the braking efficiency is due to the material softening. In Figure 21 these two phenomena are shown as Curves 1 and 2.

Curve 3 for the nickel-based material shows the drop of friction coefficient from 0.3 sharply to 0.14 at a temperature of 520°C, however the wear curve (4) remains at a low level near zero up to this temperature. The friction coefficient of Mo/LPA 100 drops from 0.2 to 0.1 around 300°C, then it stays level at 0.1 up to 600°C (Curve 5). The wear-temperature behavior (Curve 6) of Mo/LPA 100 is similar to that of nickel-based material but a little lower and a negative wear point is found at 600°C. Accordingly, the critical temperature range during which the friction significantly drops because of heavy oxidation is around 650 - 700°C for Ni vs Ni or 400 - 600°C for Mo vs Mo (Ref.8). It is evident that some additives as high temperature friction producers are needed to avoid the friction drops at relatively low temperatures for these newly-developed materials rubbed against steel.

The carbon material yields similar wear-temperature behavior (Curve 8) to the current brake material. The friction coefficient shown as Curve 7 increases from 0.2 at temperature 200°C to 0.3 at 300°C, then stays level up to 570°C. Around 575°C it drops due to material failure. It is seen that the wear increases abruptly at this temperature.

6.3.4 Effect of Velocity on Friction

The results of the friction-velocity tests are shown in Figures 22, 23, 24 for four different friction materials: one copper-based, one nickel-based, one molybdenum-based, and one carbon. The friction-velocity curves in Figure 22 remain fairly level around 0.3 to 0.4 through the whole velocity range for the conventional brake material. In Figures 23 and 24 the curves for the new materials indicate high values with very low angular speeds. In the high-speed range, however, the friction coefficients remain constantly at a low friction level, around 0.25 for the nickel-based material and 0.15 for Mo/LPA 100. This nonuniform friction-velocity relation which was also shown for the button brakes is the weak point of the newly-developed brake materials. Some improvement is needed to obtain more uniform frictional behavior.

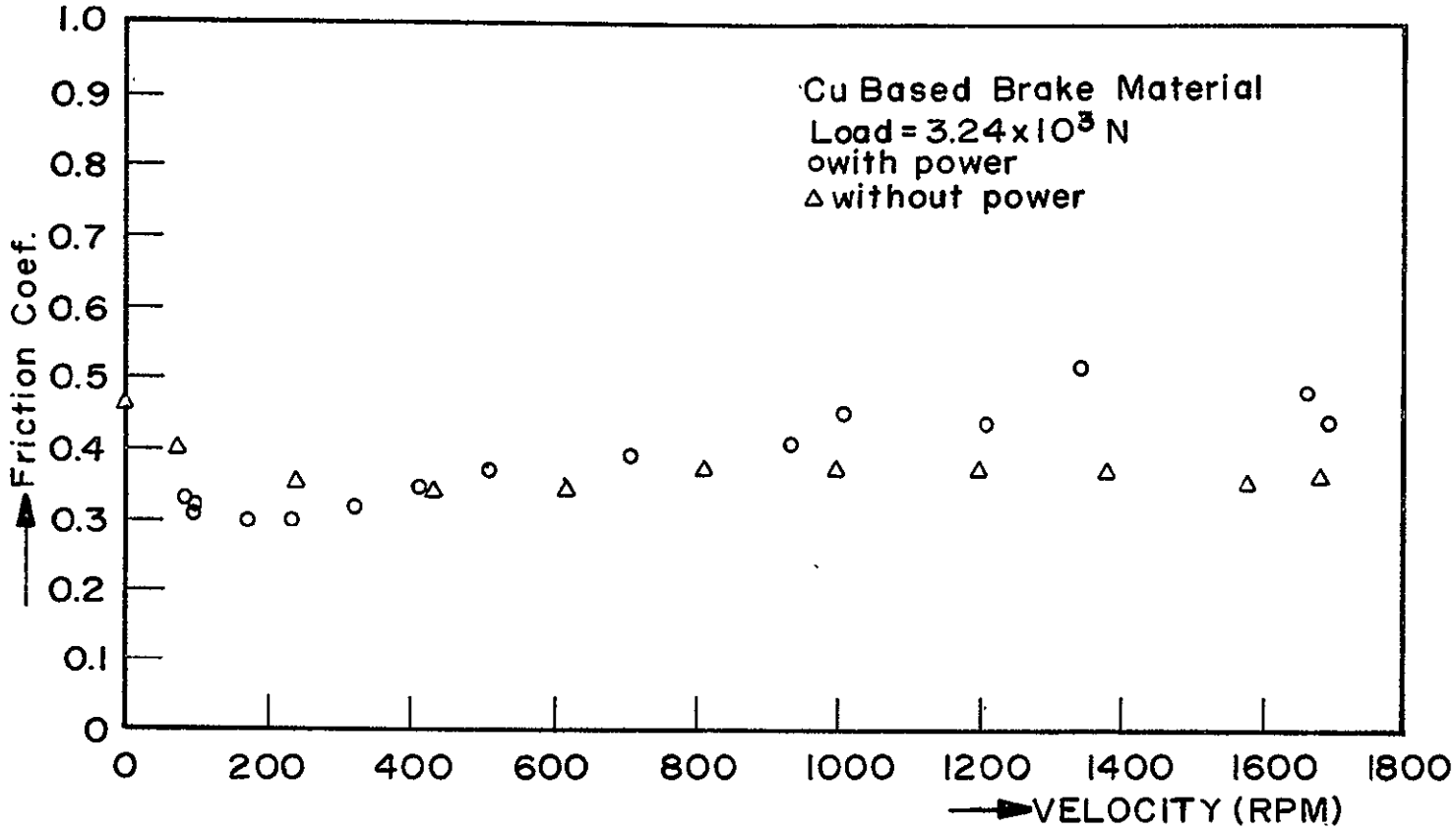

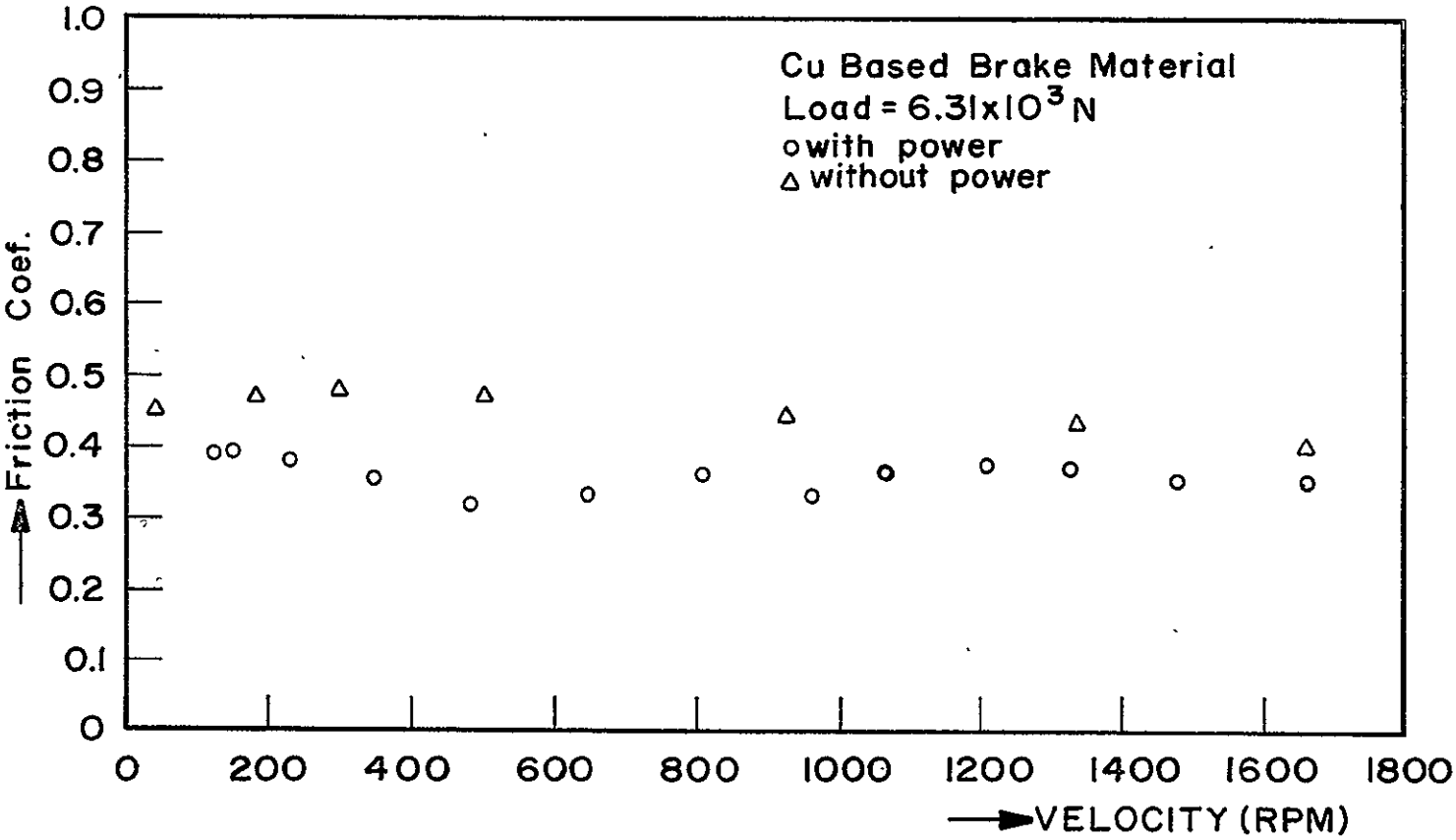

Figure 22 The Effect of Velocity on the Friction Behavior of the Copper-Based Brake Material

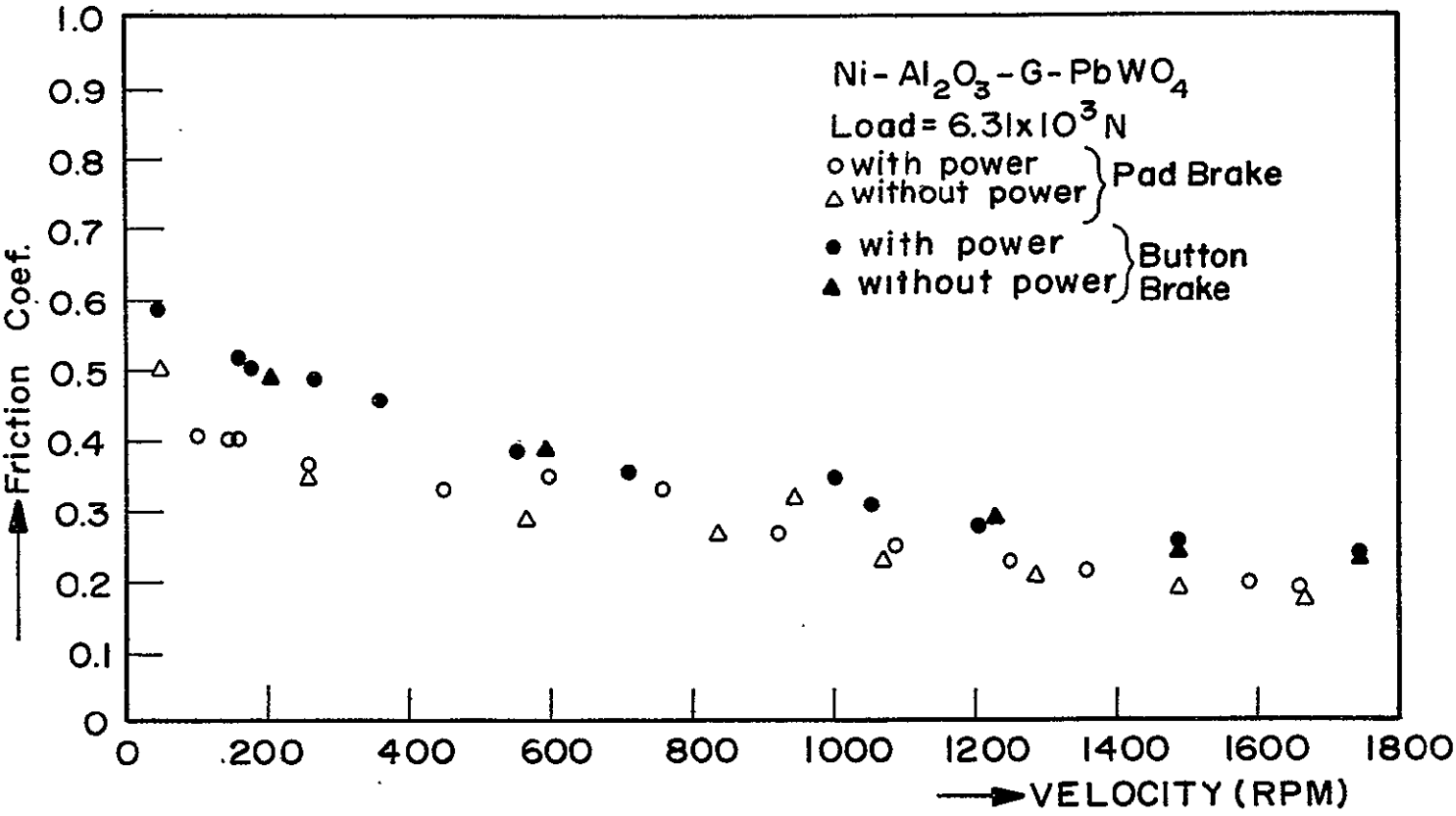

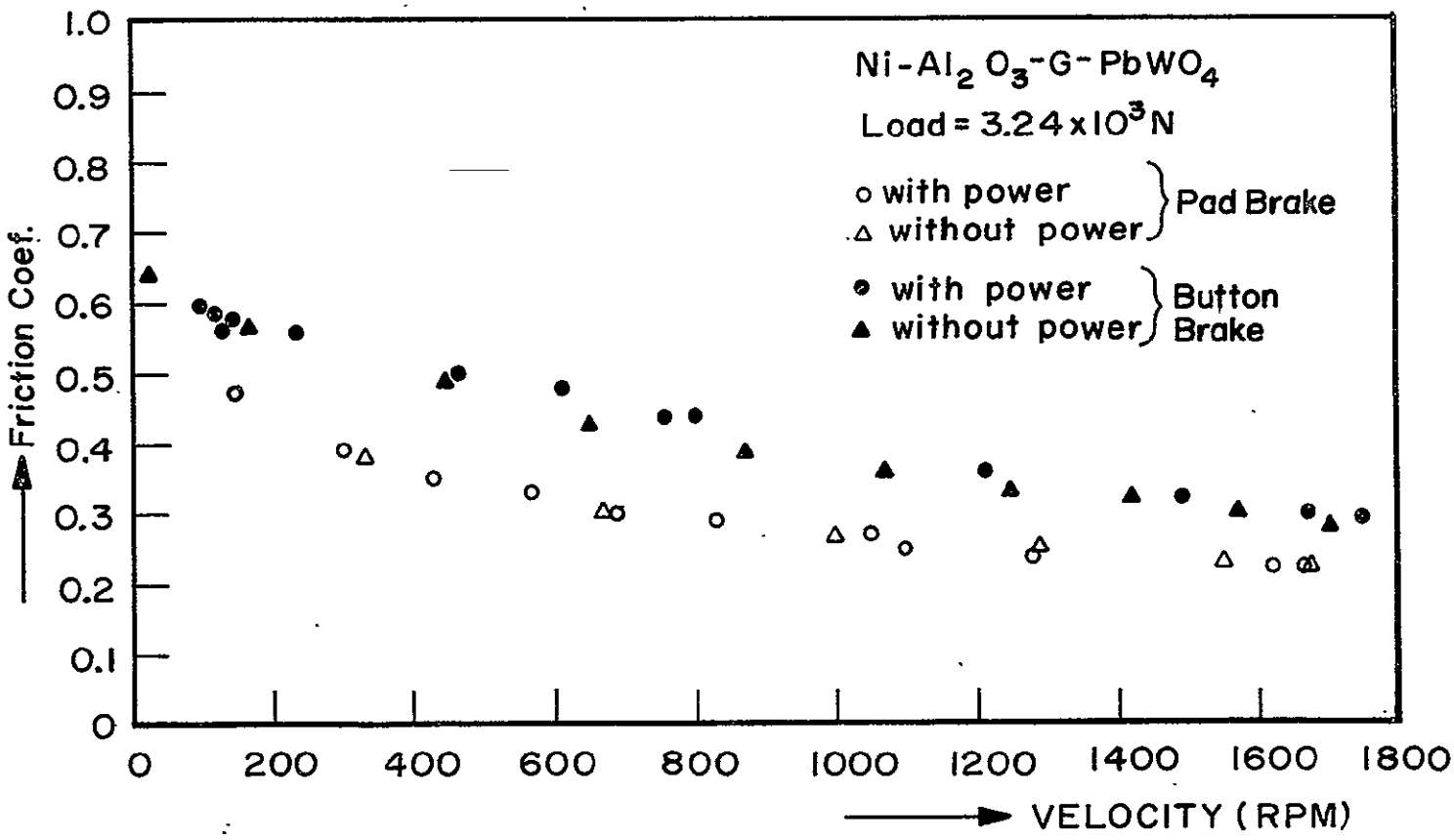

Figure 23 The Effect of Velocity on the Friction Behavior of the Nickel-Based Brake Material

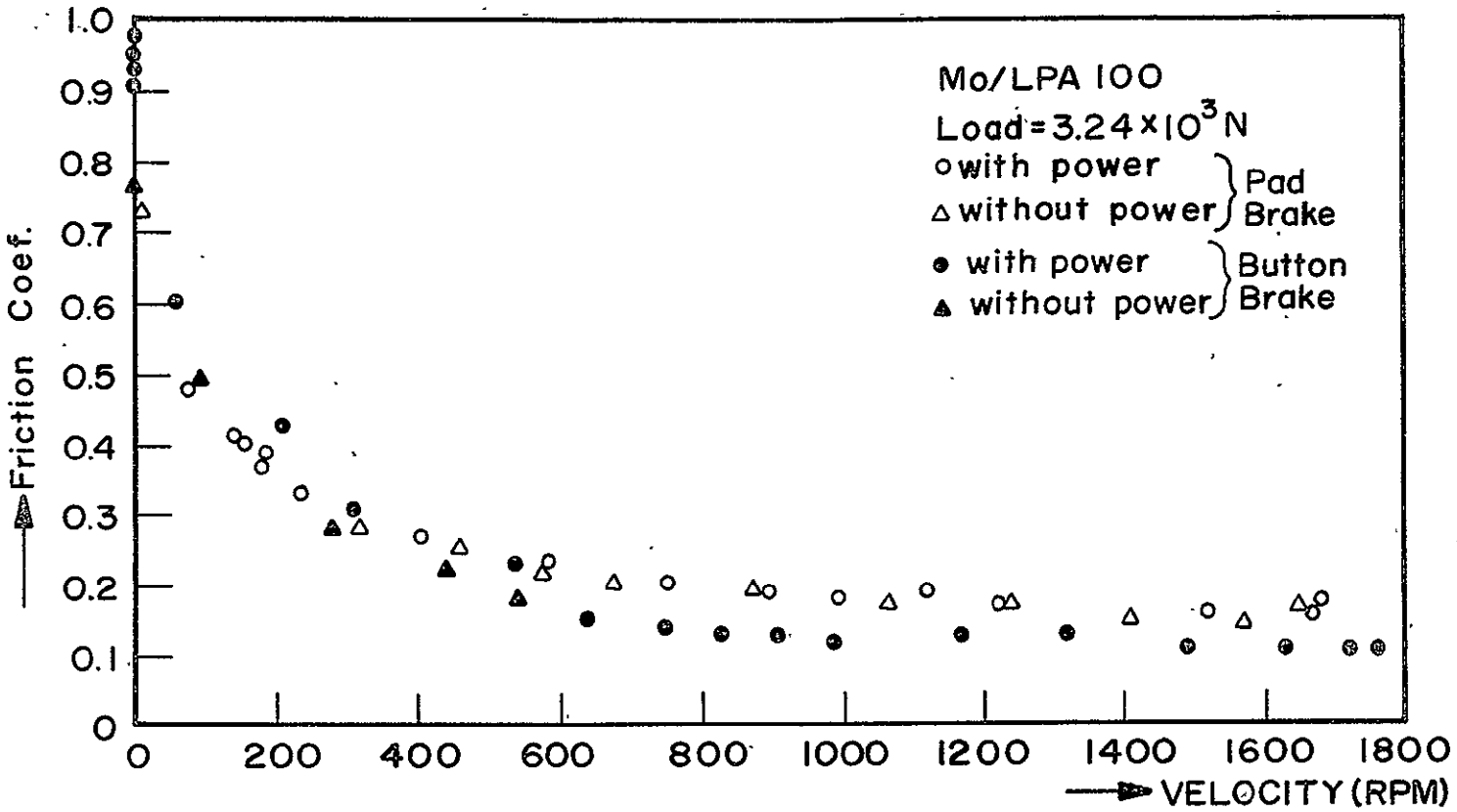

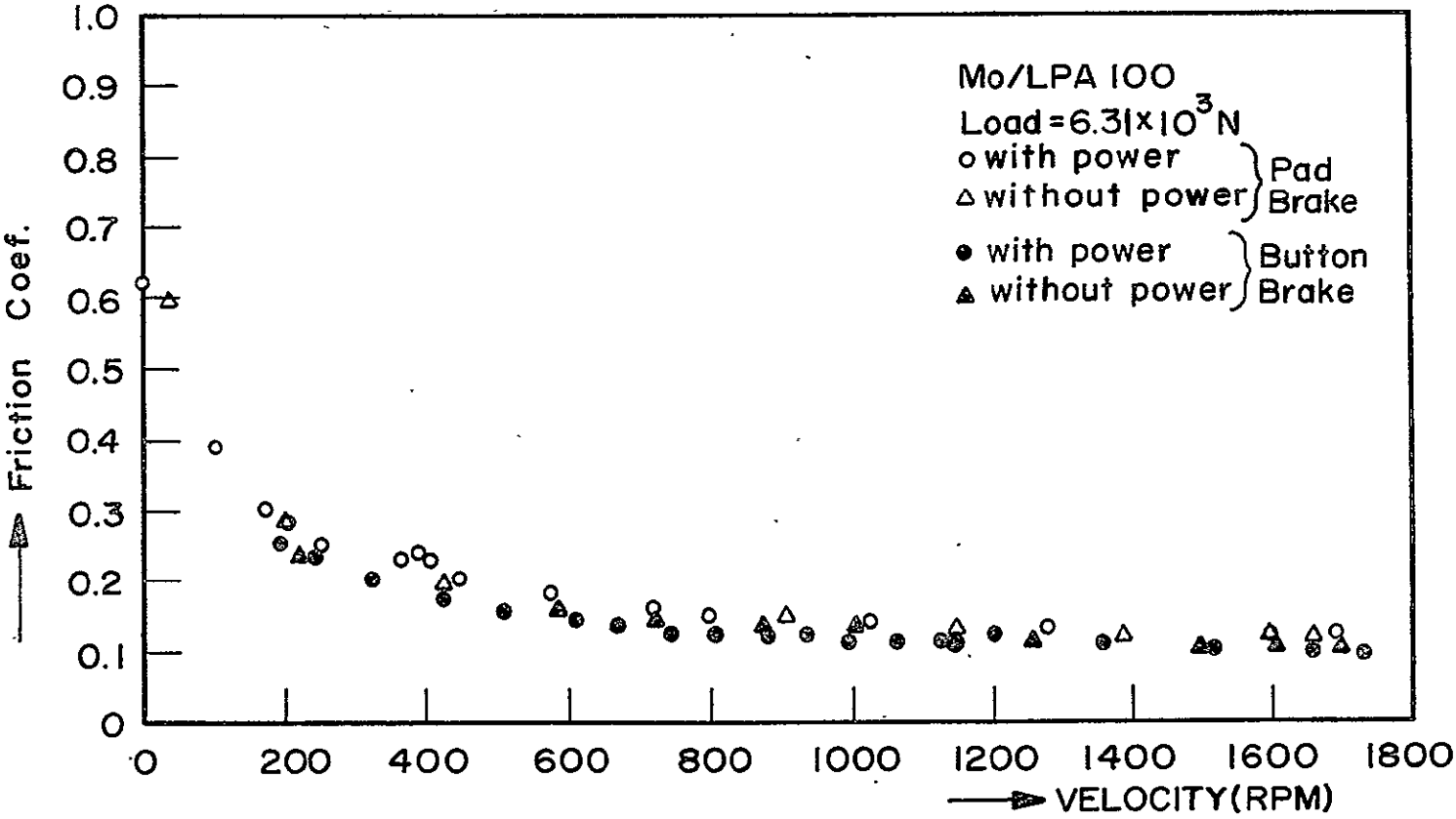

Figure 24 The Effect of Velocity on the Friction Behavior of the Molybdenum-Based Brake Material

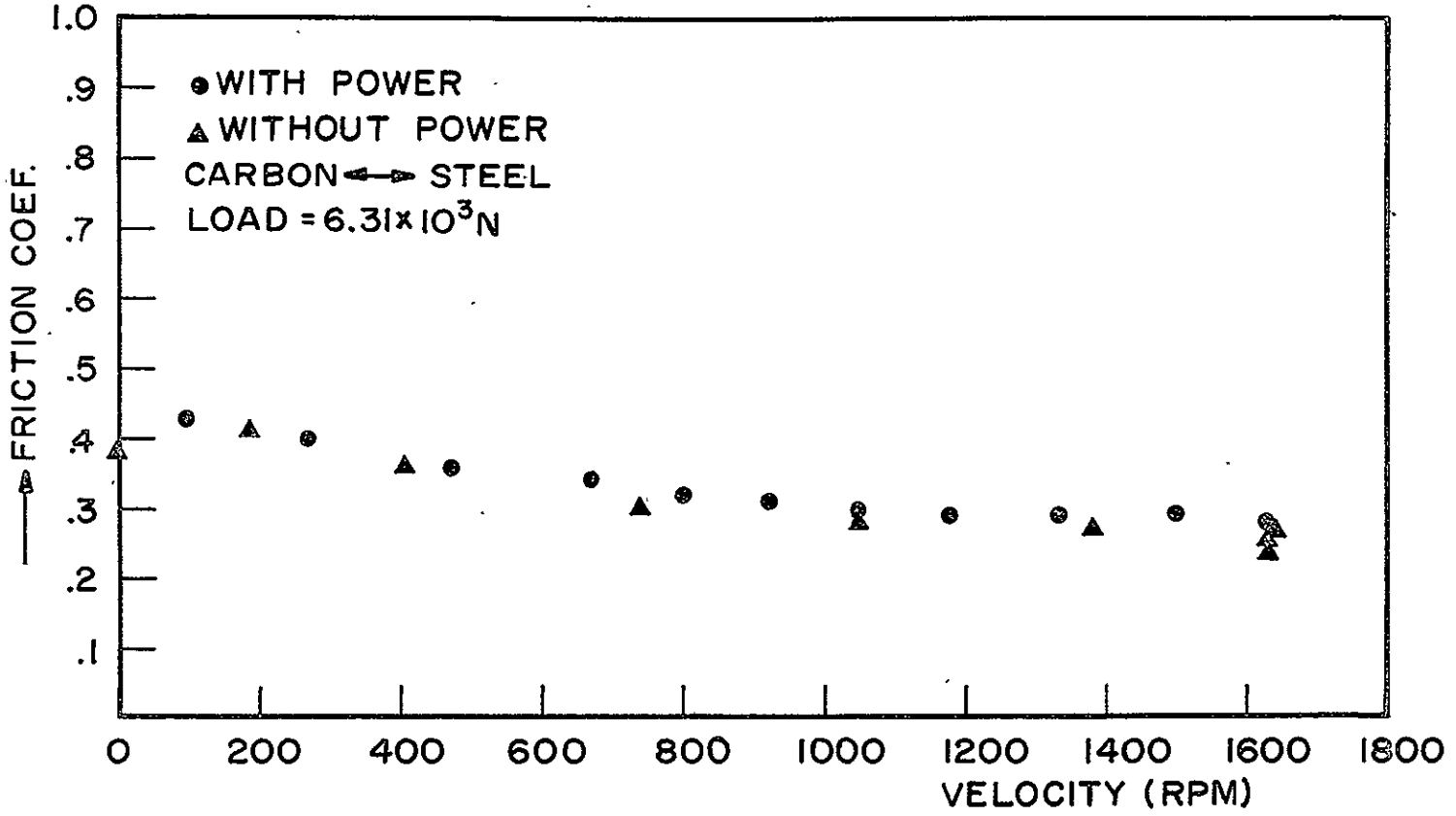

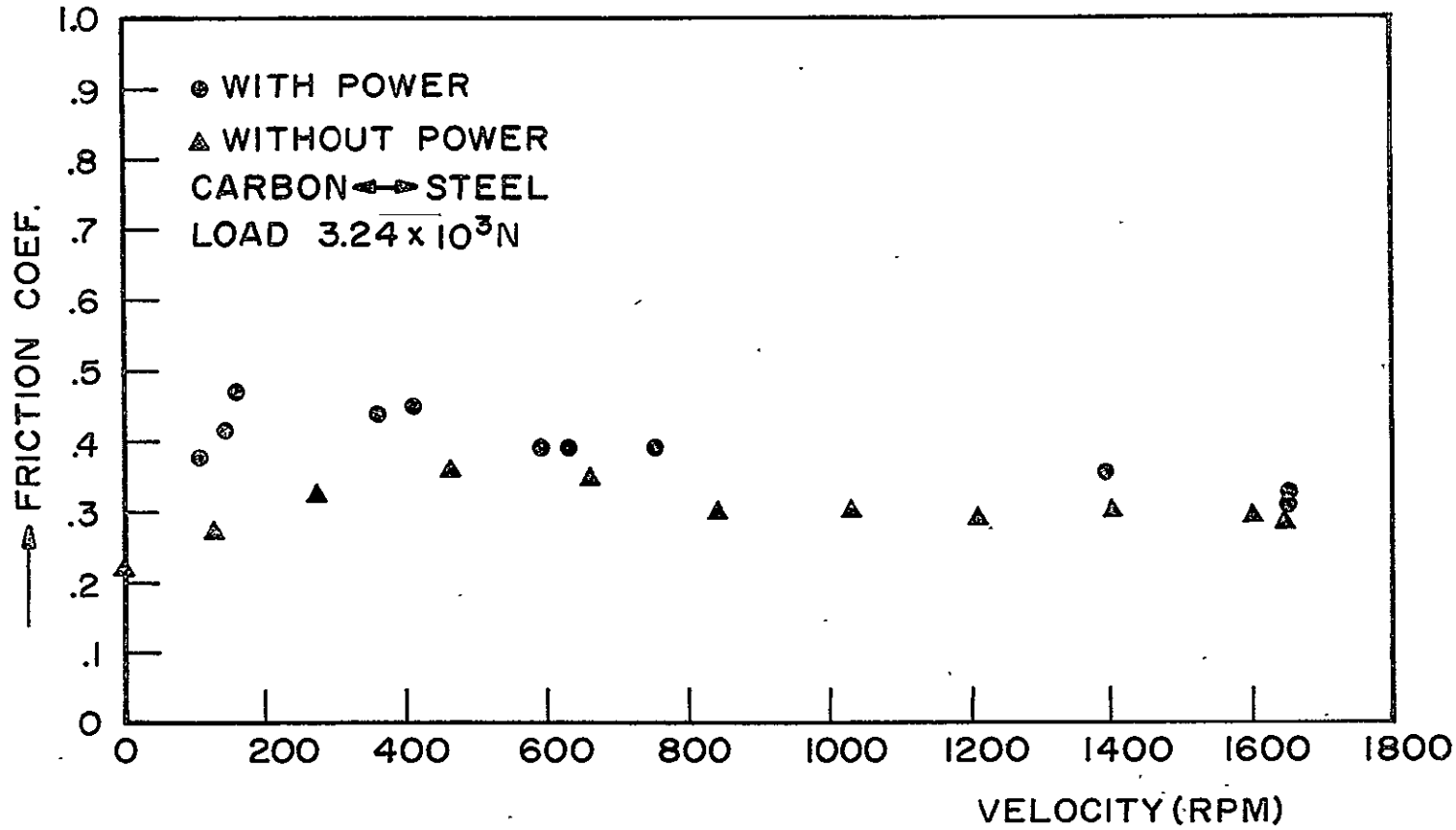

Figure 25 The Effect of Velocity on the Friction Behavior of the Carbon Material

The friction of carbon against steel stays relatively constant around 0.3 for both loading conditions (3.24 or 6.31 $\times 10^3$ N) in the speed range over 800 rpm (Figure 25). It increases when the speed is reduced from 800 rpm to around 200 rpm. Finally the friction drops when the speed is near zero value.

The effect of loading on the friction is moderate for these four materials. Generally, the high loading results only in slightly lower friction.

6.3.5 Sliding Surface Investigation

The final study of this evaluation program is a survey of the rubbed surfaces of the materials at the conclusion of all evaluation tests described previously. This is preliminary research in connection with another project on determination of the wear mechanism in high-energy brake systems. Any conclusion of this work would result in suggestion for the further improvement of the newly-developed brake materials.

The surfaces on both the lining materials and the steel disk are divided into three zones (inner, middle, and outer radii) for separate investigations on the basis of surface microstructure which relates .

1. Copper-Based Brake Material against Steel. In Figure 26, the photographs of a stator and a rotor after testing under severe conditions with the braking energy over 13 $\times 10^5$ Joules are shown. Obviously the serious oxidation formed at high temperatures on the sliding surfaces causes the excessive wear for both materials rubbed against each other. For the steel disk, special attention is paid to the middle radius portion where serious surface cracks perpendicular to the sliding direction are found. Furthermore the slotted sections were plastically deformed due to low strength at high operating temperatures. It is felt that the rotor material should also have higher temperature properties for high-energy brake performances. Though there were not many surface cracks occurring on the lining material, the thick and soft surface oxide film was formed and easily removed. This resulted in the poor wear-resistance for the current brake material at high temperatures.

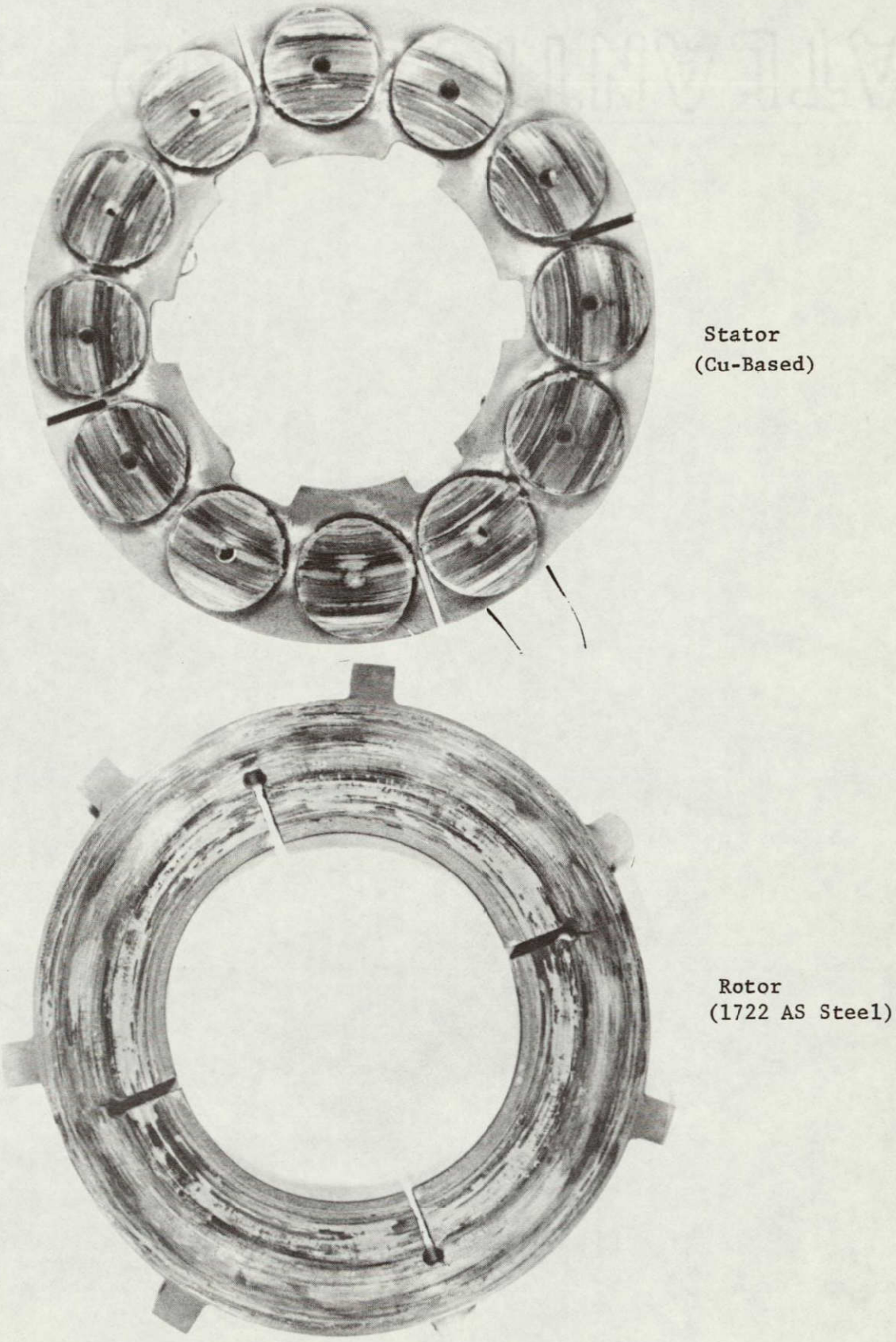

Figure 26 Photographs Showing the Rubbed Surface Conditions of a Stator with the Conventional Brake Material and a Steel Rotor after all Evaluation Tests

In Figure 27 six typical photomicrographs (50 ×) are shown illustrating both rubbed surface conditions in three zones of different radii for conventional copper-based brake material and the steel disk after all evaluation tests. There are uniformly scratched surfaces except for a few small cracks on both rubbed materials in outer radius portion. As the inspection moves inward along the radial direction, the rubbing conditions for both materials get worse due to unevenness of the loading application. The cracks grow large and deep to weaken the surface strength of both materials. It results in the scratched tracks in the middle radius portion and the isolated surface films in the inner radius zone. The isolation of surface film concentrates the contact pressure locally. Therefore the isolated surface films are much more easily cracked into pieces under higher contact pressure and worn away. Then the contact area builds up somewhere else and the processes repeat. This unbalance of surface phenomenon is the way in which the excessive wear occurs for both the copper-based brake material and the steel disk.

It is also felt that the surface conditions are similar in each radius zone for both materials rubbed against each other. But they are relatively different between three zones which were roughly specified. It means the rubbed surface conditions are only distinguished locally, especially after high-temperature rubbing.

2. Nickel-Based Brake Material against Steel. The photographs shown in Figure 28 illustrate the condition of two stators with the nickel-based material rubbed against the steel disk at the conclusion of the test. A glazy sliding film was formed on the nickel-based material except for some worn tracks which were caused by the deficiency of material bonding (may be due to the high percentage of graphite flakes included). It appears that some improvement is needed in the material bonding by either addition of some strengthening agents or improved fabrication.

Six typical photomicrographs (50 ×) shown in Figure 29 illustrate a comparison between both rubbed surface conditions in three different slide zones for the nickel-based material and the steel disk after all evaluation tests. As previously found, the rubbed surface conditions get worse along the inward radial direction. In the outer radius portion, there was little contact between the rotor disk and the nickel-based material. Here rubbing only occurred between the steel disk and the edge of steel cups which are used to hold the lining material, as indicated by the adhesion of steel cup material to the rotor.

Lining Material

Steel Disk

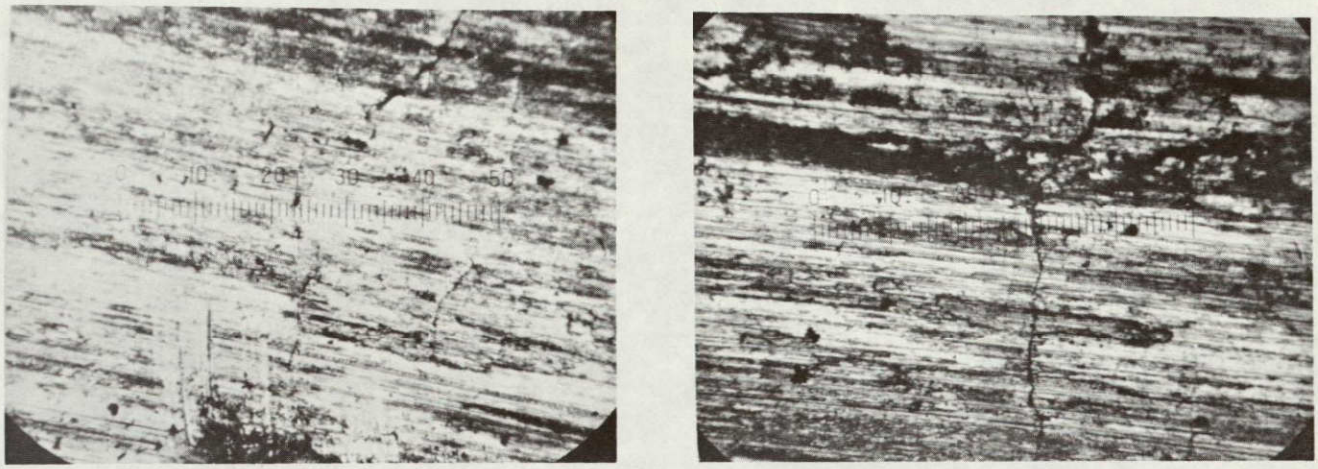

Outer Radius Zone

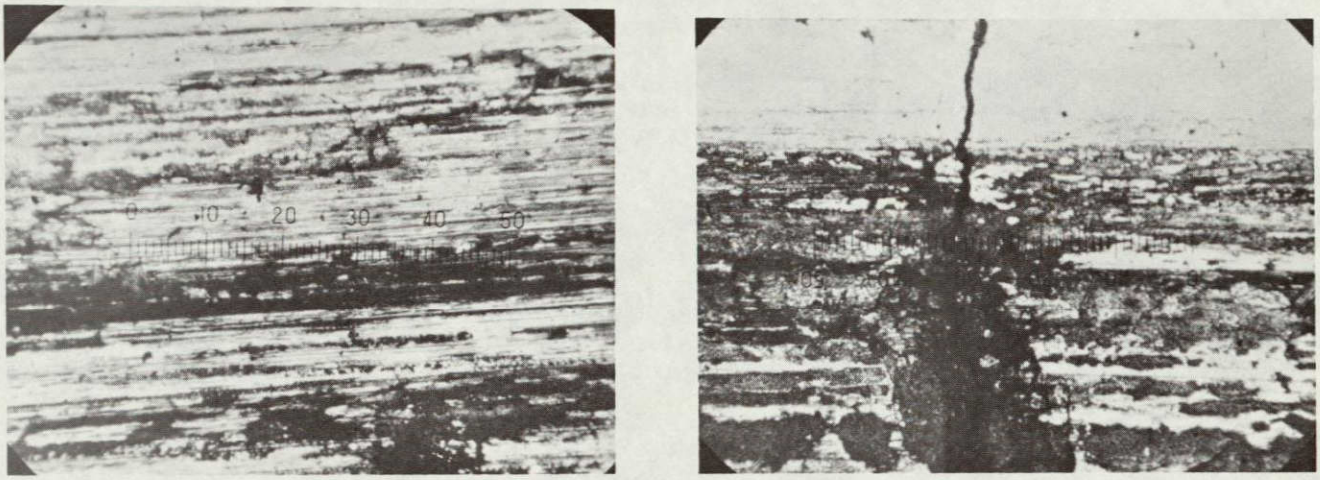

Middle Radius Zone

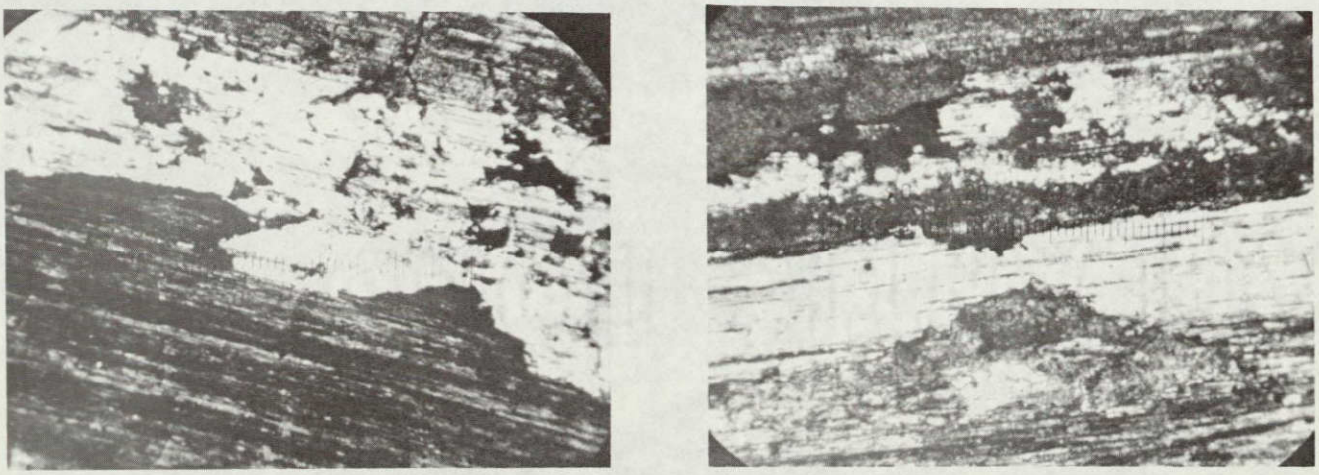

Inner Radius Zone

Figure 27 Typical Photomicrographs (50 ×) Showing Both Rubber Surface Conditions in Three Zones of Different Radii for the Conventional Brake Material and Steel Disk after all Evaluation Tests

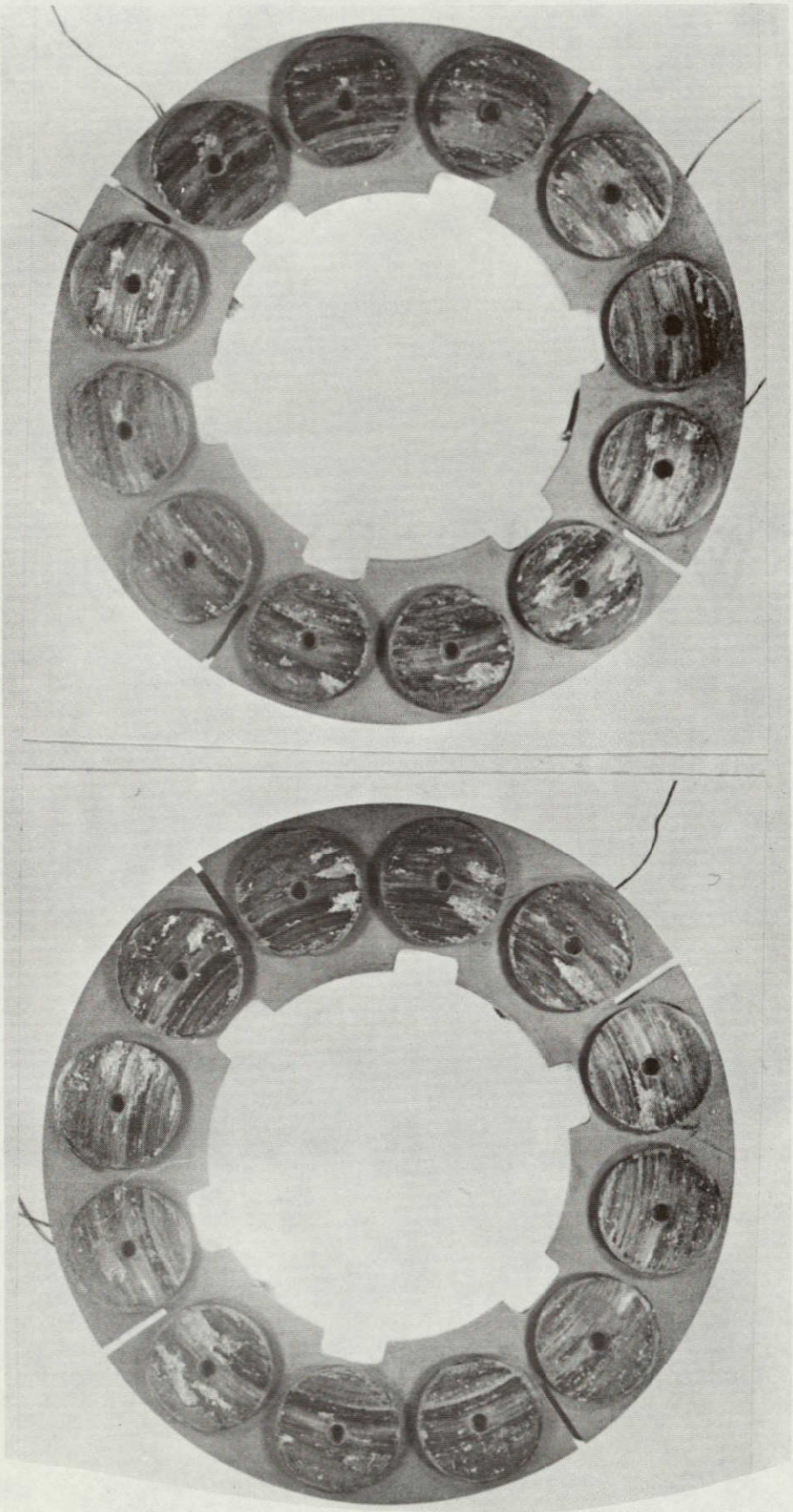

Figure 28 Photographs Showing the Rubbed Surface Condition of the Stators with the Nickel-Based Brake Material after all Evaluation Tests

Lining Material

Steel Disk

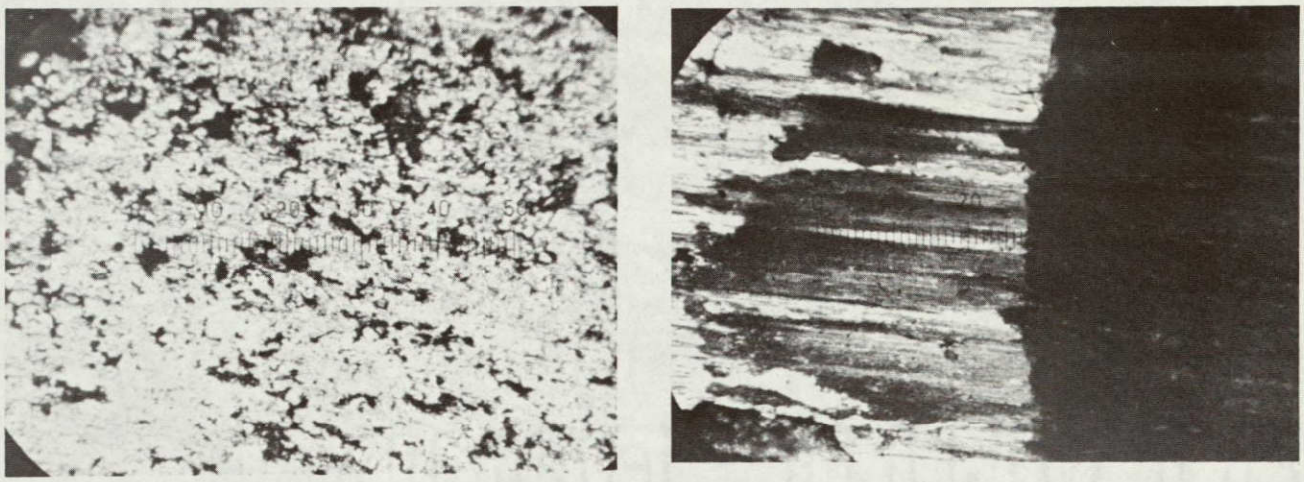

Outer Radius Zone

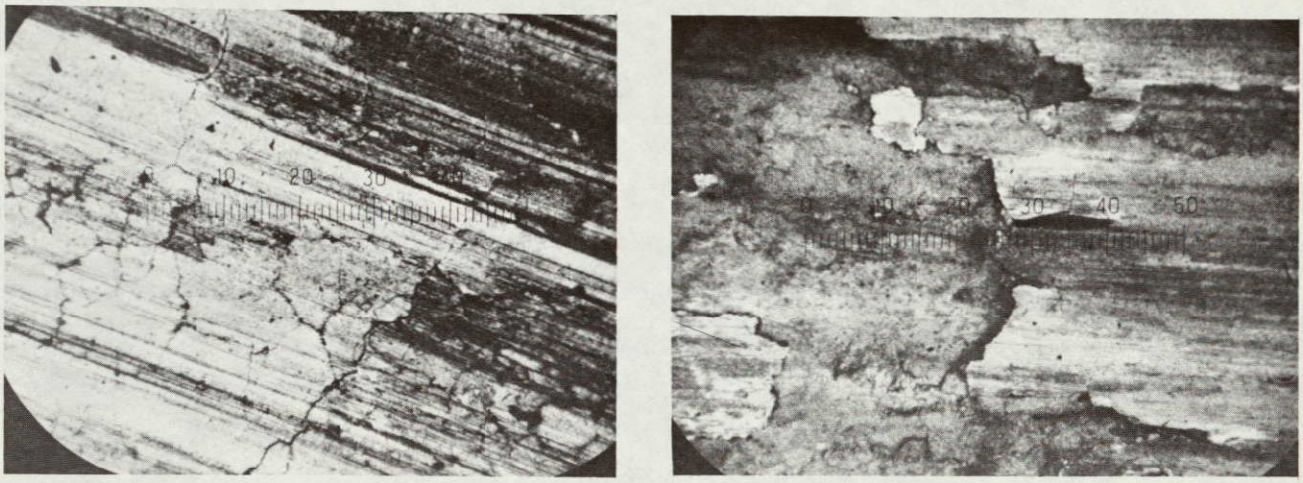

Middle Radius Zone

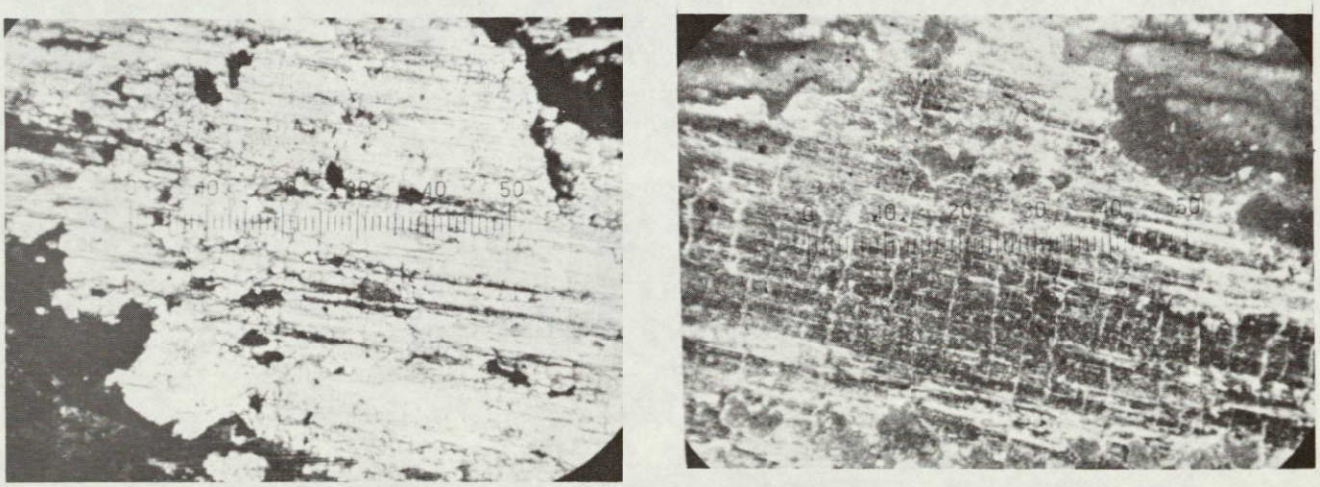

Inner Radius Zone

Figure 29 Typical Photomicrographs (50 ×) Showing Both Rubbed Surface Conditions in Three Zones of Different Radii for the Nickel-Based Material and Steel Disk after all Evaluation Tests

The next step of rubbing is shown in the middle radius zone. A sliding surface film was cracked into coarse pieces on the lining material, while on the steel disk the metal flowed to a more level situation. Finally, the sliding surface film was formed on both materials. Though it was cracked into very fine pieces, the materials were well protected from wear-off.

Obviously the rubbed surface damage of the nickel-based brake material is relatively moderate because of the formation of a glazy and stable surface film which results in the high wear-resistance for this newly-developed lining material.

3. Mo/LPA 100 against Steel. The photographs in Figure 30 illustrate the rubbed condition of a stator with Mo/LPA 100 and a steel rotor after all evaluation testing. The maximum braking energy generated in each engagement was over 13×10^5 Joules (the average surface temperature was about 600°C). It is evident that the steel became weak and soft at high temperature operations. The poor high-temperature strength resulted in the plastic deformation in the slotted sections of the steel disk. Loss of hardness caused the steel transfer especially in the inner radius zone. This steel transfer is the reason why Mo/LPA 100 gained weight at high-energy braking against steel. Thus the search for an improved high-temperature rotor material, becomes significant.

In Figure 31 there are six typical photomicrographs (50 ×) showing a comparison between both rubbed surface conditions in three different slide zones for Mo/LPA 100 and steel disk after all evaluation tests. Only light contact occurred as shown in the outer radius portion. There is no damage on the lining material. On the steel disk the rubbing tracks indicated that the sliding between steel cups and steel disk dominated in this zone. However, the isolated surface films were built up in the middle radius portion with lots of worn areas in beterrn; serious oxidation was found. In the inner radius portion the steel transfer dominated. It is felt that both surfaces are covered with similar structures of the same material which was heavily oxidized at high temperatures. Though the lining material did get worn off in the middle radius zone, the steel transfer was so severe that the total weight of stators increased through the braking under extremely high energy conditions.

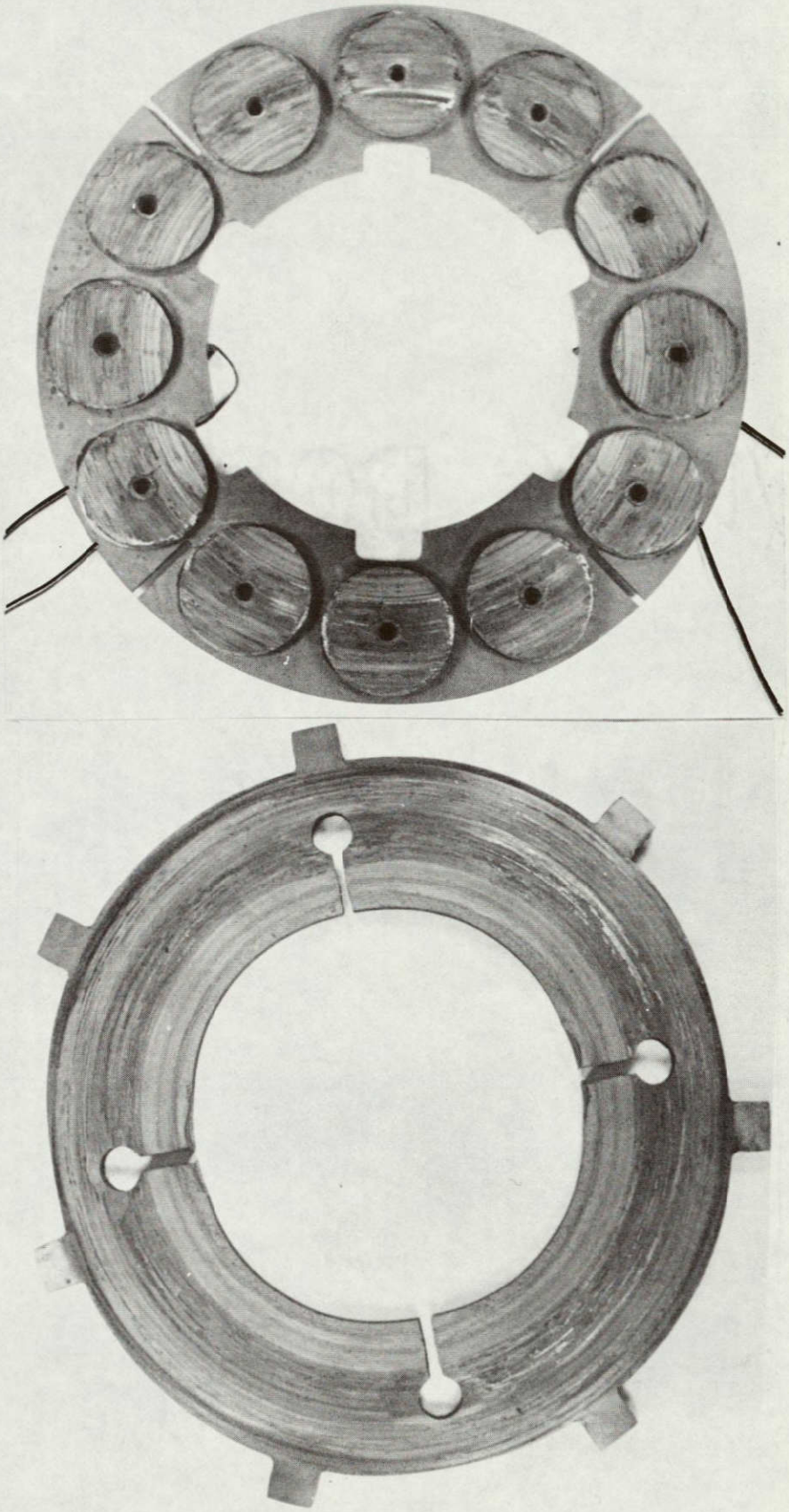

Stator
(Mo/LPA 100)

Rotor
(1722 AS Steel)

Figure 30 Photographs Showing the Rubbed Surface Conditions of a Stator with the Mo Based Material and a Steel Rotor after all Evaluation Tests

Lining Material

Steel Disk

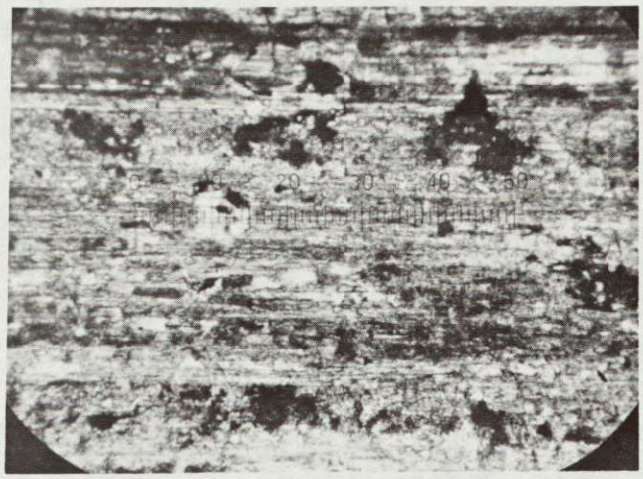

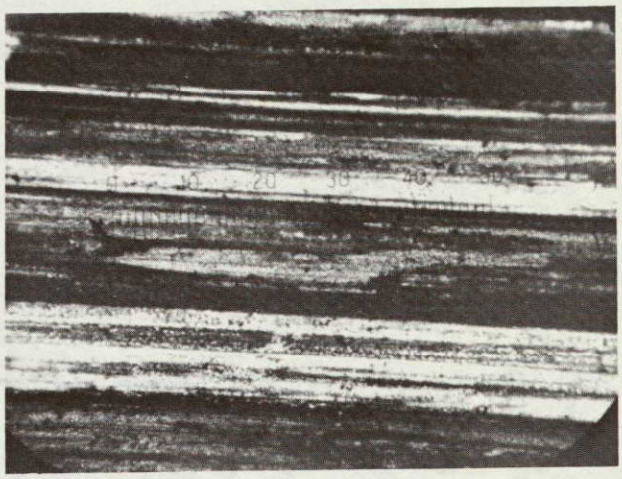

Outer Radius Zone

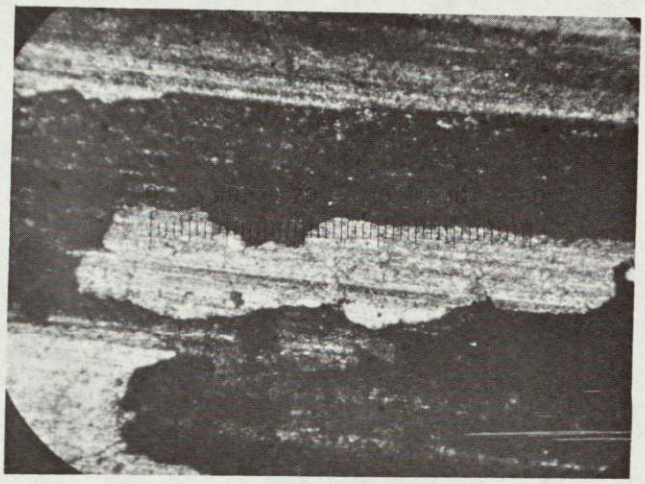

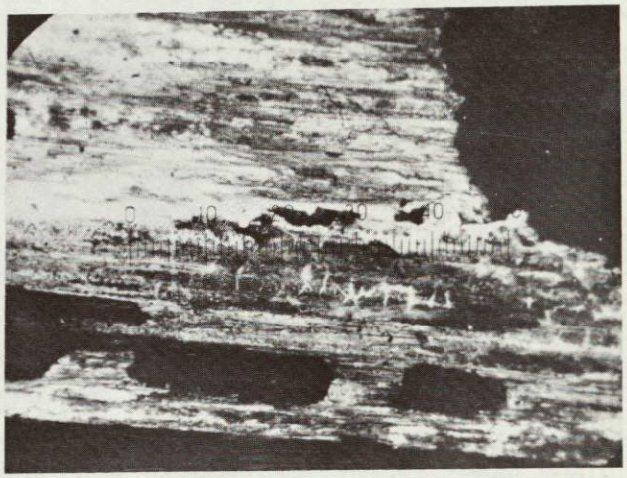

Middle Radius Zone

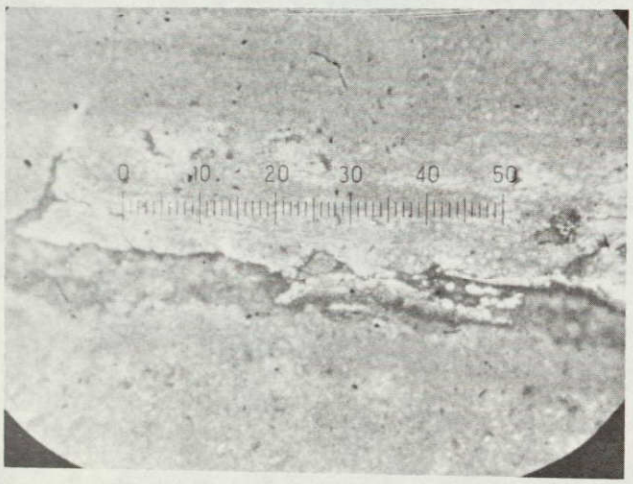

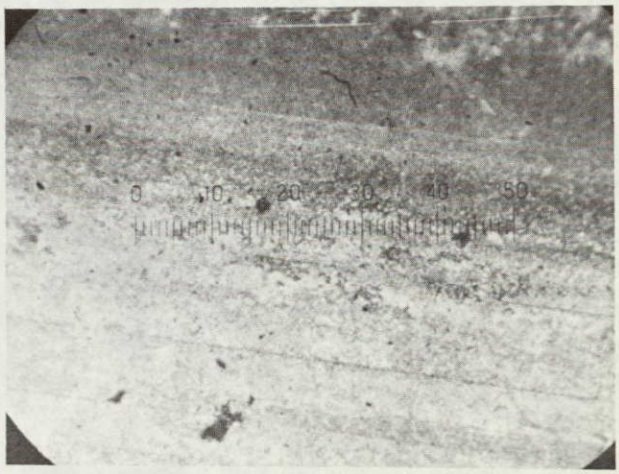

Inner Radius Zone

Figure 31 Typical Photomicrographs (50 ×) Showing Both Rubbed Surface Conditions in Three Zones of Different Radii for the Mo-Based Material and the Steel Disk after all Evaluation Tests

4. Carbon against Steel. The photographs in Figure 32 illustrate that the heavy oxidation occurred on steel surfaces and serious cracks on carbon. The material failure of carbon near the rear edge of the sliding surface results in the sharp increase of wear at high temperature performances.

These rubbed conditions are also shown in Figure 33. There are six typical photomicrographs (50×) indicating the deep cracks on carbon throughout all sliding zones and the oxide film on steel with small cracks.

Conclusion on Investigations of the Rubbed Surfaces. In concluding these investigations of the rubbed surfaces, several points can be made:

1. The relation between oxidation and wear is significant.
2. The unbalance of the shifting of isolated contacts dominates the processes of excessive wear-off for the rubbed materials.
3. The rub surface features on the lining material and on the rotor vary locally, especially after high temperature rubbing; but the two contacting surfaces are similar from the standpoint of composition and structure of the materials present on the surface.
4. Rotor materials with higher temperature properties are required.
5. It is desirable that the glazy and stable surface film formed, results in high wear-resistance for rubbing materials, especially under high-energy braking.
6. The rub interaction is adversely affected by the steel cups and the center fastener. This observation cannot be neglected in consideration of the surface phenomenon of rubbing.

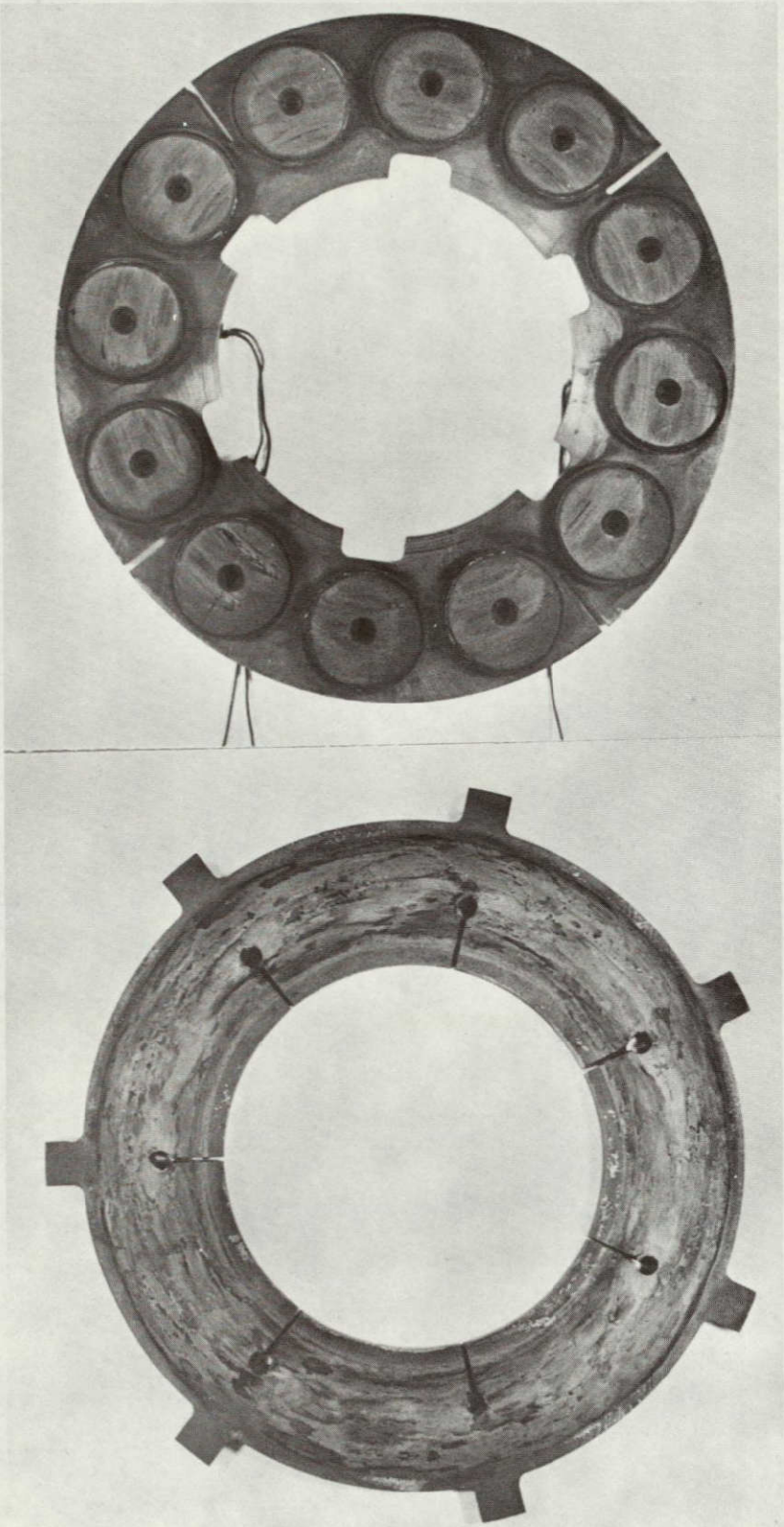

Stator
(Carbon)

Rotor
(1722 AS Steel)

Figure 32 Photographs Showing the Rubbed Surface Conditions of a Stator with the Carbon Material and a Steel Rotor after all Evaluation Tests

Lining Material

Steel Disk

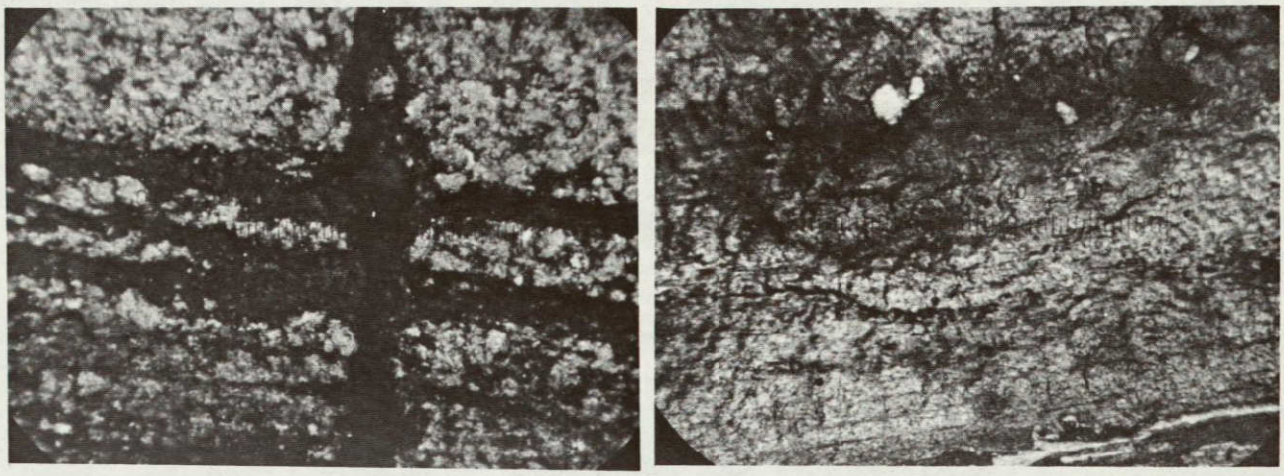

Outer Radius Zone

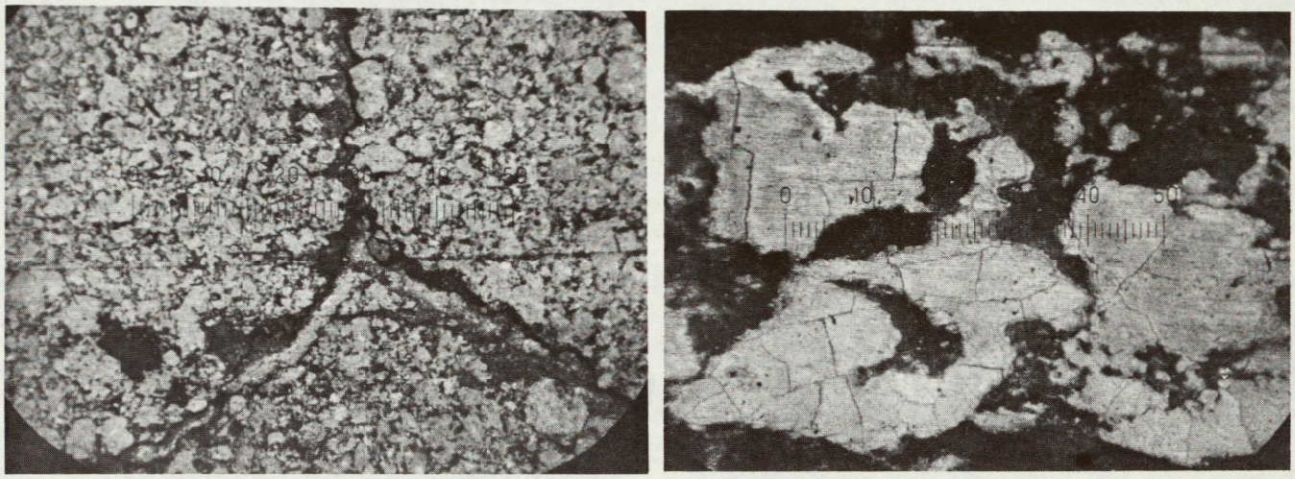

Middle Radius Zone

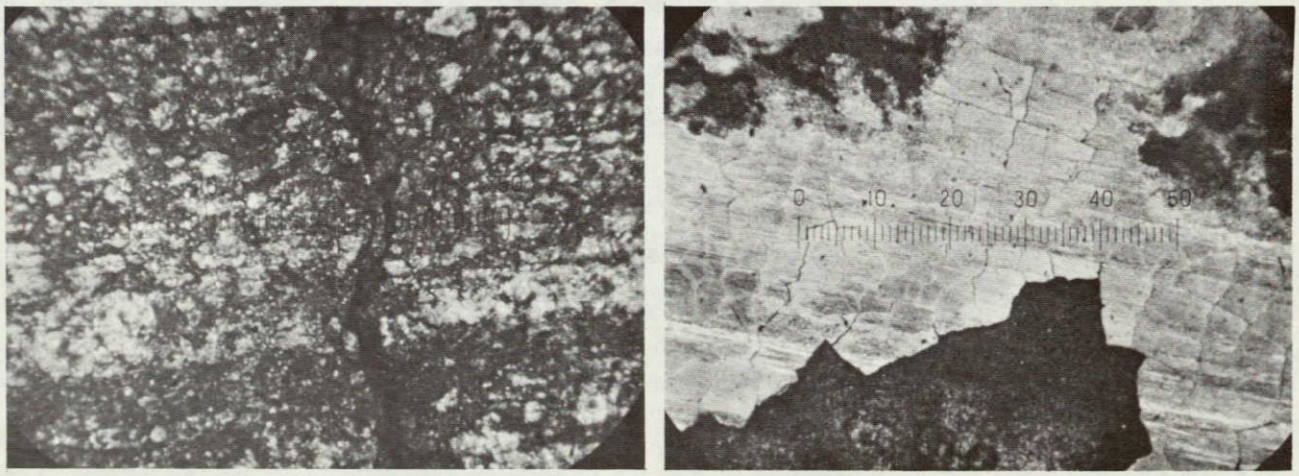

Inner Radius Zone

Figure 33 Typical Photomicrographs (50 ×) Showing Both Rubbed Surface Conditions in Three Zones of Different Radii for the Carbon Material and the Steel Disk after all Evaluation Tests

SECTION 7

SUMMARY OF RESULTS

A program has been underway to evaluate several design modifications and new materials for use in aircraft brakes. The following results have been obtained:

(1) A brake test rig has been built which will evaluate proposed high-temperature brake modifications. It is capable of operating at levels which simulate aircraft braking conditions. Energy levels of 2×10^6 Joules can be reached.

(2) Tests were run with different brake material designs (annular, slotted annular, and pads). Results using copper-based materials showed that there was little difference between them as far as friction, wear and surface temperatures are concerned.

(3) A button test geometry utilizing newly developed nickel-based and molybdenum-based materials was compared with the conventional pad design. Results showed that the button test gave higher wear.

(4) Brake tests using three new materials were compared with the conventional copper-based materials. A Ni-based and a Mo-based material showed lower wear and higher energy capacity. The low friction of the experimental materials can be compensated for by going to higher loads without a prohibitive increase in wear to either lining material or disk. Improvements, however, are needed in their friction velocity characteristics. A carbon material gave results similar to the copper-based materials.

(5) Improvements in the wear behavior of the steel rotor material are necessary before further advances in brake wear or energy capacity can be realized.

REFERENCES

1. Peterson, M.B. and Ho, T.L., "Consideration of Materials for Aircraft Brakes," NASA CR-121116, 1972.
2. Kennedy, F.E., Jr., Wu, J.J. and Ling, F.F., "A Thermal Thermoelastic and Wear Analysis of High-Energy Disk Brakes," NASA CR-134507, 1974.
3. Santini, J.J., Kennedy, F.E., Jr. and Ling, F.F., "Effect of Design Factors in Surface Temperature and Wear in Disk Brakes," Project Technical Report No.5, Tribology Laboratory, Rensselaer Polytechnic Institute, 1974.
4. Ho, T.L. and Peterson, M.B., "Development of Aircraft Brake Materials," NASA CR-134663, 1974.
5. Bill, R.C., Private communication.
6. Hooten, N.A., "Metal-Ceramic Composites in High-Energy Friction Applications," Bendix Technical Journal, Spring 1969, pp.55-61.
7. Weaver, J.V., "Advanced Materials for Aircraft Brakes," Aeronautical Journal, December 1972, pp.695-698.
8. Peterson, M.B., Floreck, J.J. and Lee, R.E., "Sliding Characteristics of Metals at High Temperatures," ASLE Transactions, Vol.3, No.1, p.101, 1960.